Medizinische Fakultät
der
Universität Duisburg-Essen

Aus der Klinik für Neurologie

Investigating the modulation of plasma IgA levels and neutrophil activation after stroke

I n a u g u r a l d i s s e r t a t i o n
zur
Erlangung des Doktorgrades der Medizin
durch die Medizinische Fakultät
der Universität Duisburg-Essen

Vorgelegt von
Ali Ata Tuz
Aus Üsküdar/Türkei
2023

DOI: 10.17185/duepublico/82318
URN: urn:nbn:de:hbz:465-20240909-092611-5

Dekan: Herr Univ.-Prof. Dr. med. J. Buer

1. Gutachter/in: Herr Univ.-Prof. Dr. med. D. M. Hermann
2. Gutachter/in: Frau Prof. Dr. rer. nat. J. Jablonska-Koch
3. Gutachter/in: Frau Priv.-Doz. Dr. phil J. Herz

Tag der mündlichen Prüfung: 25. Juli 2024

List of publications and scientific activities

Publications:

1-**Tuz, A.A.**, Hasenberg, A., Hermann, D.M., Gunzer, M., Singh, V. (2022). Ischemic stroke and concomitant gastrointestinal complications- a fatal combination for patient recovery. Frontiers in Immunology (IF:8.787) doi.org/10.3389/fimmu.2022.1037330

2-Spangenberg, P., Hagemann, N., Squire, A., Förster, N., Krauß, S.D., Qi, Y., Yusuf, A.M., Wang, J., Grüneboom, A., Kowitz, L., Korste, S., Totzeck, M., Cibir, Z., **Tuz, A.A.**, Singh, V., Siemes, D., Struensee, L., Engel, D.R., Ludewig, P., Melo, L.M.N., Helfrich, I., Chen, J., Gunzer, M., Hermann, D.M., Mosig, A. (2023). Rapid and fully automated blood vasculature analysis in 3D light-sheet image volumes of different organs. Cell Reports Methods (IF: 3.8) doi.org/10.1016/j.crmeth.2023.100436

3-Cibir, Z., Hassel, J., Sonneck, J., Kowitz, L., Beer, A., Kraus, A., Hallekamp, G., Rosenkranz, M., Raffelberg, P., Olfen, S., Smilowski, K., Burkard, R., Helfrich, I., **Tuz, A.A.**, Singh, V., Ghosh, S., Sickmann, A., Klebl, A.K., Eickhoff, J.E., Klebl, B., Seidl, K., Chen, J., Grabmaier, A., Viga, R., Gunzer, M. (2023). ComplexEye - a multi lens array microscope for High-Throughput embedded immune cell migration analysis. Nature Communications (accepted) (IF:17.7)

Oral and poster presentations:

11/2022, 21st Day of Research of the Medical Faculty, Univ. of Duisburg-Essen, Essen
Poster presentation: Peyer's Patch B cells undergo cell death via neutrophil-released DNA after tissue injury

09/2022, Joint Meeting DGfl and ÖGAI, Hannover
Oral Presentation: "Stroke differentially impacts immune cells loss in systemic and intestinal lymphoid organs"

Awards:

11/2022, Best Poster Award, 21st Day of Research of the Medical Faculty, Univ. of Duisburg Essen

Table of Contents

1. Introduction

1.1 Stroke Epidemiology

Stroke is a major health concern worldwide, with significant morbidity, mortality, and disability. It is the second leading cause of death globally and according to recent statistics, approximately 17 million people suffer from stroke each year, with over 6 million deaths resulting from this condition (Feigin et al., 2016) . In addition to its high mortality rate, stroke also results in significant long-term disability and related healthcare costs.

Stroke incidence and prevalence vary among different populations, with some groups being more susceptible to this condition than others. Globally, the incidence of stroke is estimated to be around 13.7 million cases per year, with a prevalence of 116 million cases (Collaborators, 2021). The incidence of stroke is higher in high-income countries, yet the prevalence is higher in low- and middle-income countries, reflecting the lower survival rates and higher morbidity associated with stroke in these regions. In the United States, stroke incidence has been declining over the past few decades, with an estimated annual incidence of 610,000 cases (Benjamin et al., 2019). Despite this decline, stroke remains a major public health concern due to its high morbidity and mortality rates.

The incidence and prevalence of stroke are influenced by various risk factors, including modifiable and non-modifiable risk factors. Some of the modifiable risk factors include hypertension, diabetes, smoking, physical inactivity, and unhealthy diet. Non-modifiable risk factors include age, gender, race/ethnicity, and family history of stroke. Hypertension is the most important modifiable risk factor for stroke, accounting for up to 48% of all strokes (Collaborators, 2021). Other modifiable risk factors such as diabetes, hyperlipidemia, smoking, and physical inactivity play significant roles in increasing the risk of stroke. Yet, several studies have shown that targeting these risk factors through lifestyle modifications can reduce stroke incidence and improve outcomes (O'Donnell et al., 2016).

Age is a significant non-modifiable risk factor for stroke, with the incidence of stroke

increasing with age. In the United States, over 75% of all strokes occur in individuals aged 65 years and above (Benjamin et al., 2019). In addition to age, gender and ethnicity also play a role in stroke risk. Men have a higher incidence of stroke compared to women, although women have a higher mortality rate from stroke (Benjamin et al., 2019).

1.2 Stroke Comorbidities and Complications

Identifying factors related to poor functional status among stroke survivors is crucial, as they can increase the risk of hospitalization, mortality, and early death and align with the overall goal of rehabilitation services (Gaynor et al., 2018). Stroke survivors commonly have comorbid conditions, particularly older patients, with clinical strokes occurring without comorbidities in less than 6% of cases (Nelson et al., 2017). The coexistence of multiple chronic conditions and comorbidity patterns may arise due to shared risk factors and pathophysiology (e.g., heart disease and stroke) or causal/precursor relationships (e.g., atrial fibrillation and stroke). Previous community-based studies have shown that the burden and patterns of multimorbidity are associated with impaired physical functioning, reduced quality of life, and higher utilization of healthcare services (Aubert et al., 2022, Pati et al., 2019).

Commonly shown by multiple studies, hypertension, diabetes, hyperlipidemia, and obesity, which are the main components of metabolic syndrome, are established risk factors for cardiovascular diseases, including stroke (Marshall et al., 2015). This finding supports a previous systematic review that identified the major multimorbidity pattern of cardiovascular-metabolic diseases in adult populations (Prados-Torres et al., 2014). These above-mentioned metabolic diseases are among the most prevalent comorbidities among stroke patients (Aubert et al., 2022, She et al., 2022). Metabolic syndromes are prominent risk factors in the development of stroke, making them common comorbid diseases among patients with stroke.

When combined, hypertension and hyperlipidemia account for the most common comorbidities and risk factors of stroke. Hyperlipidemia, a condition characterized by elevated levels of lipids or lipoproteins in the blood, is a significant comorbidity in stroke patients. It is an important risk factor for ischemic stroke, as previously shown in large

clinical trials or patient registries, ≈45% to 60% of patients exhibit elevated serum cholesterol levels (Sacco et al., 2008). Furthermore, higher serum cholesterol levels at presentation to emergency unit with stroke were correlated with a worse final outcome after treatment (Restrepo et al., 2009). Interestingly, stroke risk shows differential interactions between the thrombotic course of stroke pathophysiology- large artery atherosclerosis and related stroke events showing more correlation with higher lipid levels, as shown by a case-control study (Yaghi and Elkind, 2015). Yet, lacunar strokes showed contrary correlations with hyperlipidemia- some case-control studies showing higher lacunar stroke risk with higher total cholesterol or LDL levels, whereas other studies showing no relation between cholesterol and lacunar stroke. Several genetic and epigenetic conditions with environmental factors may play a role in this differential regulation, yet, preclinical studies have shown pathophysiological explanations to stroke-hyperlipidemia relation, that will be explained in the following chapters.

In patients with hyperlipidemia, statins are recommended to prescribe to lover blood lipid levels. The Stroke Prevention by Aggressive Reduction in Cholesterol Level and Treat Stroke to Target studies have shown that statins are beneficial for patients with stroke without additional statin related adverse effects (Stroke Prevetion by Aggressive Reduction in Cholestrol Levels et al., 2008). Beneficial effect of statins was observable in patients using them before and/or after stroke onset. This suggests that managing hyperlipidemia could potentially improve outcomes in long term among stroke patients. Furthermore, risk of recurrent stroke decreases with usage of statins. However, statin effectiveness starts approximately after 4-6 weeks of treatment, in which alternative and more short-term effective medications might be considered. In addition to statins, alternative medications like Gemfibrozil are also available to patients, but further studies are needed for better optimization of treatment paradigms. In contrary, studies have suggested that hypolipidemia, but not hyperlipidemia, is a risk factor for small vessel diseases such as intracerebral hemorrhages, microbleeds, white matter hyperintensities, and perhaps, lacunar infarction1. Hence, in the current clinical setting, most benefit is achieved via targeting stroke-free individuals with higher risk of cardiovascular events and by aiming at optimal blood lipid levels without moving in the edges of hypo- or hyperlipidemia.

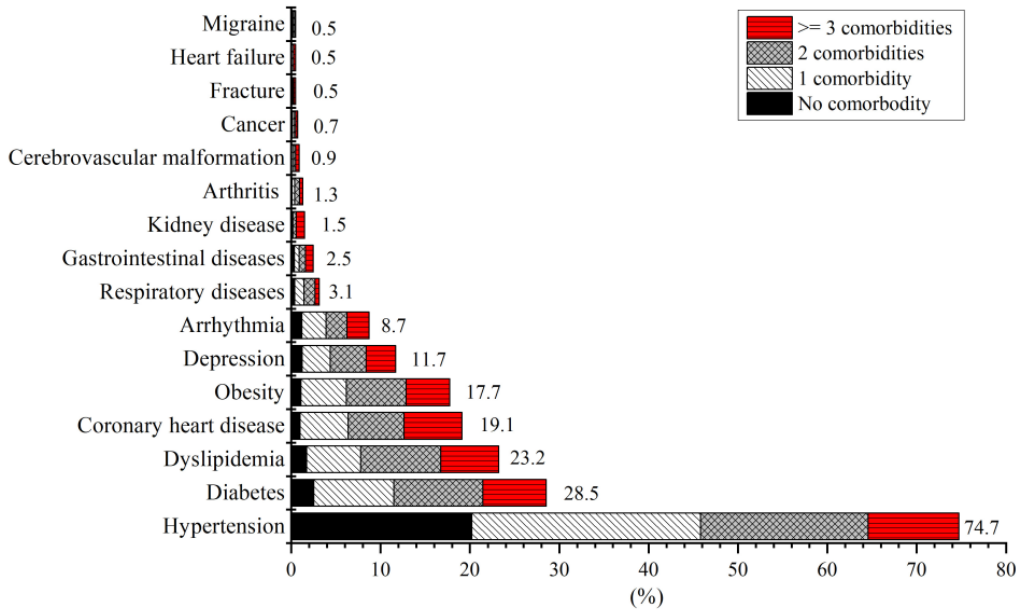

Figure 1: Stroke comorbidities are usually present in combination among patients (She R., et al., Front. Aging Neurosci., 2022)

Most of the stroke patients present with more than one comorbidity (Fig 1). For instance, most of the patients with hyperlipidemia or diabetes present with at least one additional comorbidity. Furthermore, a study found that diabetic patients who have suffered a stroke are more likely to have hyperlipidemia than those without diabetes (16% vs. 8%, respectively)2. This indicates that hyperlipidemia is not only common among stroke patients but also more prevalent in certain subgroups of these patients. On the other hand, high-density lipoprotein (HDL) was shown to promote angiogenesis via vascular endothelial growth factor activation in a preclinical model, yet, more studies are needed to understand the effects in humans with dyslipidemia (Jin et al., 2018). As a result, in admission, a thorough analysis needs to be made to cover all possible comorbidities and to provide best care.

Hyperlipidemia is also commonly observed with hypertension in patients suffering stroke. Hyperlipidemia causes endothelial damage, thus leading to loss of vasomotor activity. This might cause elevated systemic blood pressure, namely hypertension. Moreover, some prospective studies have shown higher plasma lipid levels being correlated with future hypertension development. Hypertension is the most commonly observed comorbidity in stroke patients and the underlying supportive effect of hyperlipidemia is also crucial in understanding the pathophysiology. As stroke is a

complex disease with multiple contributors, hyperlipidemia might be one of the most important risk factors causing more frequent stroke, leading to hypertension and more burden in patients.

In addition to cardiovascular comorbidities, many stroke patients have commodities related to the gastrointestinal system, infections and depression. Previous research has frequently reported close associations between gastrointestinal diseases and affective disorders in both, general and clinical populations (Mayer, 2000). Acute life-threatening stressors and central nervous system mechanisms play significant roles in the development of gastrointestinal and psychiatric symptoms. It is worth noting that the separate pattern of cardiovascular and gastrointestinal diseases was not commonly observed in previous studies, indicating a potential role of gut microbiota on cardiovascular, as well as nervous systems. Furthermore, the burden and patterns of comorbidity are associated with both poor physical and cognitive function in patients with acute ischemic stroke. These findings have implications for the proper management of comorbidities among stroke patients in order to maintain and improve post-stroke physical and cognitive functioning outcomes. Therefore, assessments of comorbidity should be routinely included in stroke research and clinical practice (Collaborators, 2021).

As a result of multiple predispositions of stroke patients to several different diseases, stroke can result in various complications, depending on the location and severity of the stroke. To better analyze, stroke complications can be classified as neurological and non-neurological complications. Some of the common complications of stroke include neurological deficits, cognitive impairment, depression, and social isolation. Neurological deficits such as paralysis, weakness, and speech difficulties are common after a stroke and can significantly affect the patient's quality of life. Cognitive impairment, including memory loss, attention deficits, and executive dysfunction, also occurs in a significant proportion of stroke survivors (Merriman et al., 2018). Depression is another common complication of stroke, with up to 33% of stroke survivors experiencing depressive symptoms (Towfighi et al., 2017).

In addition to neurological deficits, stroke patients also exhibit a wide range of non-neurological complications, including gastrointestinal tract (GIT) disturbances,

immunosuppression, and bacterial infections throughout all recovery periods, from the hyper-acute to chronic phases (Collaborators, 2021). These complications impose a significant burden on patients' overall health and significantly impede post-stroke brain recovery. Furthermore, GIT complications are the leading cause of increased morbidity and mortality in patients (Fu, 2019). The post-stroke deterioration of intestinal epithelial barriers may facilitate the invasion of lumen bacteria into systemic tissues and activate immune cells (Hu et al., 2022). Several studies have demonstrated GIT disturbances in stroke patients, such as dysphagia, gastrointestinal bleeding, or constipation (Rofes et al., 2018). A recent stroke registry study showed that 19.6% of patients experience swallowing problems and indicate a dysphagia frequency of 75.4%, which is associated with a high risk of death during hospital admissions (Bonkhoff et al., 2022). In patients suffering from brain stem infarcts, dysphagia and paralytic ileus-induced constipation are the two most prevalent symptoms, with an overall incidence rate of 45%. Among these, 30% exhibited a delay in proximal colonic transit (Li et al., 2017, Roth et al., 2020). Inversely, a history of constipation is associated with poorer stroke outcomes, and the administration of laxatives has been found to elevate stroke risk in constipated patients (Tan et al., 2021). Moreover, elderly individuals with pre-existing GIT disorders such as dysbiosis, hypertension, diabetes mellitus, and intestinal infections are at an increased risk of future ischemic stroke (Roth et al., 2020). This large-scale patient data suggests that gastrointestinal complications may pre-exist prior to a stroke event and may contribute to an increased stroke incidence. The derived correlation could be attributed to the fact that these complications are also major comorbidities in cerebrovascular diseases. GIT bleeding is diagnosed in approximately 0.1-8.4% of stroke patients and is associated with high mortality rates (Fu, 2019, Xia et al., 2019). GIT bleeding is also an independent risk factor for recurrent stroke, indicating a bidirectional interaction between the intestine and brain (Du et al., 2020). Furthermore, patients with large cortical infarcts exhibit more severe gastrointestinal symptoms that significantly correlate with poorer outcomes (Arnold et al., 2016, Fu, 2019). Despite early diagnosis, erythrocyte transfusion, and endoscopic interventions, there are no approved therapies against GIT bleeding, necessitating careful patient diagnosis in hospitals (Haak et al., 2021). Pneumonia, in addition to other comorbidities, occurs mostly within the first week after stroke. Aspiration pneumonia is one of the most common reasons, caused by the lack of coughing

and gag-reflex after stroke. Furthermore, several studies show different pathophysiological explanations, such as decreased salivation and swallowing caused oral microbiota dysbiosis; bacterial dissemination from gastrointestinal tract into lungs or parasympathetic system related immunosuppression. However, there is no defined diagnostic risk assessment method validated in the clinics (Grossmann et al., 2021).

Urinary tract infections are also one of the other immunosuppression related clinical pictures, worsening stroke outcome (PoissonJohnston and Josephson, 2010). Further reasons also include frequent use of urinal catheters among patients with stroke, and bladder dysfunction as a result of nervous system damage.

Complications after stroke are highly common and increase the mortality and morbidity. Early interventions might lessen the adverse effects and increase life quality of the patients. Yet, there is still need for better definitions for early diagnosis and better treatments. This could be possible via better understanding of stroke pathophysiology both in short and long term after stroke.

1.3 Stroke Pathophysiology

Stroke pathophysiology involves the processes and mechanisms that lead to the development of cerebral ischemia or hemorrhage, which makes it imperative to understand the underlying concepts to develop effective management and prevention strategies.

The pathophysiology of stroke encompasses the mechanisms and processes that result in cerebral ischemia or hemorrhage, necessitating a comprehensive understanding of the underlying concepts to develop effective management and prevention strategies (KumarSelim and Caplan, 2010). Stroke occurs when blood flow to the brain is disrupted, either due to blockage of an artery, termed ischemic stroke, or rupture of blood vessels leading to hemorrhage, termed hemorrhagic stroke (KumarSelim and Caplan, 2010). The brain requires a continuous supply of oxygen and glucose for normal functioning; thus, any disruption to blood flow leads to cellular damage and death within minutes, with permanent neuronal injury occurring within hours (DirnaglIadecola and Moskowitz,

1999). Once the blood supply is compromised, the affected cells quickly become hypoxic and experience metabolic insufficiency, leading to an accumulation of neurotransmitters such as glutamate, which induces excitotoxicity and neuronal death (Kane and Ward, 2021).

The pathology of stroke can be divided into three main stages: acute ischemia, infarction, and secondary injury (DirnaglIadecola and Moskowitz, 1999). Among these, acute ischemia occurs when the brain is deprived of blood supply, leading to a cascade of events that ultimately lead to cell death. The pathophysiology of acute ischemia is complex but essentially involves a combination of two interrelated processes: reduction in cerebral blood flow (CBF) and metabolic dysfunction. CBF can be reduced due to a variety of factors, including thrombosis, embolism, or vasospasm. These processes can cause progressive arterial occlusion, leading to a decrease in CBF and consequent hypoxia, acidosis and accumulation of toxic metabolites (DirnaglIadecola and Moskowitz, 1999). Ischemia leads to a decrease in cellular ATP production and accumulation of lactic acid, ultimately resulting in a shift to anaerobic metabolism. This shift in metabolism leads to an accumulation of reactive oxygen species (ROS) and oxidative stress, further exacerbating cellular damage (DirnaglIadecola and Moskowitz, 1999). Additionally, the decreased production of ATP leads to the failure of the Na+/K+ ATPase associated with the plasma membrane, which results in increased intracellular sodium ions and extracellular potassium ions. This disrupts the balance between intracellular and extracellular ions, leading to cellular depolarization and the release of neurotransmitters, most notably glutamate (Kane and Ward, 2021). Glutamate is an excitatory neurotransmitter that plays a key role in stroke pathophysiology. The accumulation of glutamate leads to excessive activation of N-methyl-D-aspartate (NMDA) receptors causing a rapid influx of calcium ions into the cell, leading to calcium overload and hyperexcitability of neurons. This process can initiate a cascade of events, including the activation of various enzymes such as protein kinase C (PKC), phospholipase A2 (PLA2), and sphingomyelinase. These enzymes contribute to the breakdown of cell membranes, producing free radicals and reactive oxidants, leading to further cell death (Kane and Ward, 2021).

After acute ischemia, in the infarction stage, the initial insult results in the onset of localized brain tissue damage, which is called the infarct core while in hemorrhagic stroke

it is called the hematoma. This tissue damage leads to the release of a cascade of inflammatory cytokines and the influx of immune cells such as microglia, neutrophils and macrophages which leads to the development of secondary injury (DirnaglIadecola and Moskowitz, 1999). Secondary injury is the final stage of stroke pathophysiology and involves a range of processes that increase the extent of neuronal damage beyond the initial infarct site. Secondary injury involves both excitotoxic and neuroinflammatory processes which contribute to recruitment and activation of immune cells peak in inflammatory responses further perpetuating excitotoxicity. Such processes all contribute to amplification of initial ischemic or hemorrhagic insult also result in detrimental effects. Therefore, stroke pathology involves multiple interrelated molecular and cellular processes that ultimately result in cellular death and brain tissue damage. Understanding the underlying mechanisms that contribute to this condition is critical for developing effective therapies and management strategies. In particular, treatments that target the early stages of stroke may offer promising benefits in terms of reducing the extent of neuronal injury and preventing long-term disability. Moreover, research efforts that aim to identify new molecular targets involved in stroke pathophysiology may provide opportunities for more effective interventions in the future.

1.4 Stroke Treatment

The acute treatment options for stroke include thrombolysis and mechanical thrombectomy. Long-term treatment for stroke involves medication therapy, rehabilitation, and lifestyle changes. Effective stroke treatment requires a multidisciplinary approach, involving neurologists, physical therapists, occupational therapists, and other healthcare professionals. Patients who receive timely and appropriate treatment for stroke have a higher chance of recovery and improved quality of life.

1.4.1 Acute Treatment

The acute treatment of stroke involves emergency medical care aimed at minimizing brain damage and preventing further complications. At this stage, quick intervention is necessary to eliminate any obstacles to blood flow to the brain. The two primary acute treatments for stroke include thrombolysis and mechanical thrombectomy.

According to the current stroke treatment guidelines, upon admission, patient's current status is determined via National Institutes of Health Stroke Scale (NIHSS) score, which shows the severity of stroke. Afterwards, a computerized tomography (CT) scan is made to observe the infarct and also the possible perfusion deficits, that might me reversible. CT scan is preferred, as it visualizes the blood flow deficits better and takes only a few minutes to process and interpret. This detection and visualization processes are then followed by thrombolysis, if disabling deficit is present and there are no contraindications against the therapy. Thrombolysis is a medical procedure that involves the administration of clot-busting drugs such as tissue plasminogen activator (tPA) to dissolve the blood clot in the brain(Berge et al., 2021). According to the European Stroke Organisation (ESO), using thrombolysis within 3-4.5 hours after the onset of stroke symptoms can improve outcomes and reduce disability. However, tPA therapy may carry risks, such as bleeding in the brain, and must be carefully monitored by medical professionals. Additionally, tPA administration requires a screening protocol to ensure that it is safe to use in a patient (Berge et al., 2021, Alamowitch et al., 2023).

Possible and relatively common contraindications include the usage of anticoagulation or previous history of spontaneous bleeding. These explained procedures are normally done as quick as possible after symptom onset, 4.5 hours being the limit for thrombolysis therapy. Yet, recent clinical trials showed that when a patient has perfusion mismatch in CT, it is beneficial to treat with thrombolysis up to 24 hours after symptom onset (Alamowitch et al., 2023, Dawson et al., 2022).

Mechanical thrombectomy is a medical procedure that involves removing clots from the brain using specialized devices inserted through the femoral artery. The devices are used to grab and remove the clot from the blood vessel, allowing free blood flow to the brain. This type of treatment is typically performed on patients whose symptoms have persisted

longer than the recommended time for tPA administration or those who have clots too large to dissolve through tPA therapy. Another clinical picture is, when a patient has proximal artery closure, it is recommended to prefer thrombectomy, after eliminating contraindicatory situations (Turc et al., 2023). As a result, “time is brain” is the current motto for acute stroke treatment with two main possibilities and new results about time constraints.

1.4.2 Subacute to Chronic Treatment

Subacute to chronic treatment for stroke aims to prevent recurrent strokes, minimize disabilities, and improve quality of life via controlling comorbidities. The primary long-term treatment options for stroke include medication therapy, rehabilitation, and lifestyle changes (She et al., 2022).

Medication therapy involves the administration of drugs aimed at managing underlying conditions that increase the risk of stroke, such as hypertension, high cholesterol levels, and diabetes. Antiplatelet agents such as aspirin or clopidogrel are used to prevent the formation of blood clots in the vessels. If there is an indication, such as atrial fibrillation, Factor Xa inhibitors are prescribed as anticoagulants to prevent clots from forming in the heart. Furthermore, statins are used against high levels of cholesterol; antihypertensive and antidiabetic medications are selected according to patients’ disease history (Dawson et al., 2022). Patients usually start taking these medications directly at the stroke unit, in which a thorough investigation for the reason and underlying factors of stroke is made. As some of these medications need monitoring at the beginning, it is also beneficial for the patients to get used to taking them at the stroke unit under supervision. Furthermore, the medications might need some time to have metabolic effects, that is why, life style modifications and avoidance of the underlying conditions are fundamental in subacute and chronic treatment.

Rehabilitation is another long-term treatment option for stroke that focuses on helping stroke survivors regain their physical, cognitive, and emotional abilities. Rehabilitation may include both physical therapy and occupational therapy. Physical therapy is used to

help stroke survivors regain physical movement and strength, while occupational therapy focuses on restoring daily living skills and cognitive function (Quinn et al., 2021).

Stroke rehabilitation is aimed at minimizing the long-term disabilities and complications associated with stroke. Rehabilitation can involve various interventions, including physical therapy, occupational therapy, speech therapy, and cognitive rehabilitation. Physical therapy is aimed at improving mobility and reducing muscle weakness, while occupational therapy focuses on improving daily activities such as dressing, feeding, and grooming. Speech therapy is aimed at improving speech and language function, while cognitive rehabilitation targets memory, attention, and problem-solving skills.

Rehabilitation after stroke can be challenging due to the wide range of complications and disabilities associated with this condition. However, several studies have shown that early and intensive rehabilitation improves outcomes and reduces long-term disabilities.

Lifestyle changes are also essential in the long-term management of stroke. A healthy lifestyle that includes regular exercise, a balanced diet, and avoiding smoking and excessive alcohol consumption can help reduce the risk of recurrent stroke. Patients with stroke should also receive education on recognizing the warning signs of stroke to seek prompt medical attention if symptoms reoccur.

1.5. Animal Models

Strokes is a heterogeneous disease, including several subtypes and affecting different arteries and brain regions in different groups of patients. However, there are common pathophysiological characteristics that can be mimicked in in vivo models. Hence animal models are essential tools to mimic these processes for investigating pathophysiology and therapeutic approaches in different time frames and different severities of stroke (Li and Zhang, 2021).

Rodent models offer several advantages for studying ischemic stroke. They are relatively easy to breed, handle, and house, making them cost-effective and widely available. Their genomes can be easily manipulated through genetic engineering techniques, allowing researchers to study specific molecular pathways involved in the pathogenesis of

ischemic stroke. Moreover, rodents share many physiological and anatomical features with humans that are relevant to stroke, such as the presence of a dense network of collateral vessels and similar cerebrovascular anatomy (Matur et al., 2022).

Despite their utility, rodent models present certain limitations in the study of stroke. The diminutive size of these animals restricts the capacity to evaluate neurological deficits, potentially failing to represent the full range of complications observed in human stroke patients. Moreover, the rodent brain exhibits a greater extent of collateral circulation relative to humans, introducing potential confounders when appraising the effectiveness of therapeutic interventions (Matur et al., 2022, Li and Zhang, 2021).

1.5.1. Transient Middle Cerebral Artery Occlusion

Transient middle cerebral artery occlusion (tMCAO) is a widely used animal model that mimics clinical stroke. In the tMCAO model, a filament is inserted into the middle cerebral artery to block blood flow, and then it is removed after a defined period of occlusion, allowing reperfusion. This model mimics the clinical scenario of a thrombotic or embolic stroke with reperfusion, which is more common than completely occlusive strokes (DirnaglIadecola and Moskowitz, 1999). The model is particularly useful because it closely mimics the clinical features of stroke, including the sudden onset of neurological deficits and the presence of ischemic damage in the brain, further followed by reperfusion injury. During tMCAO, blood flow to the brain is temporarily interrupted, which leads to a decrease in oxygen and glucose supply to the affected area. This results in the death of brain cells and the development of ischemic damage. The extent of the damage depends on the duration of the occlusion and the severity of the resulting ischemia. The tMCAO model has been used to study a wide range of stroke-related topics, including the role of inflammation in stroke, the effects of neuroprotective agents, and the mechanisms of stroke recovery. The model has also been used to test potential treatments for stroke, including thrombolytic agents and neuroprotective drugs (Liu and McCullough, 2014). One advantage of the tMCAO model is that it allows researchers to study the effects of stroke in a controlled environment. Another advantage of the tMCAO model is that it allows researchers to study the effects of stroke over time. The model can be used to

induce stroke at different time points, which allows researchers to study the acute and chronic effects of the condition. This can help to identify the mechanisms that contribute to stroke recovery and to develop interventions that promote recovery. In conclusion, transient middle cerebral artery occlusion is a widely used animal model that mimics clinical stroke.

Animal models of ischemic stroke have contributed significantly to our understanding of the pathophysiology of the disease and the development of new therapies. As a result of these models, we now know that ischemic stroke pathobiology involves a complex interplay between multiple cellular and molecular mechanisms, such as excitotoxicity, oxidative stress, inflammation, and apoptosis (LakhanKirchgessner and Hofer, 2009). Furthermore, researchers have identified numerous targets for stroke therapy, such as anti-inflammatory agents, anti-oxidant compounds, neuroprotective agents, and cell-based therapies.

1.5.2. Mimicking Clinics- Western Diet

Western Diet (WD) has been widely studied in animal models to understand their effects on various health conditions, including stroke. These diets include different percentages of fat, carbohydrate and protein levels, compared to normal foods supplied for mice under housing conditions. In addition, higher percentage of fat and salt in this diet type mimics the Western diet type of humans (Hintze et al., 2018).

Animal models are often used to study the effects of high-fat diets on the brain and to identify potential mechanisms that may contribute to the development of stroke. Studies have shown that high-fat diets can lead to the development of obesity, insulin resistance, and other metabolic disorders in animal models (Hintze et al., 2018). These conditions are known to increase the risk of stroke and other cardiovascular diseases in the clinics (She et al., 2022). WD has also been shown to increase oxidative stress and inflammation in the brain, which can contribute to the development and worse prognosis of stroke (Sharifi-Rad et al., 2020). The results of these studies may depend on the type of animal model used, the duration of the diet, and other factors. For instance, in addition to wild

type (WT) mice, Apolipoprotein E (ApoE) knockout mice are used in combination with WD to induce severe obesity with metabolic syndrome in mice, as these mice lack ApoE, which is a lipid homeostasis regulator (Herz et al., 2015). Even though this model has higher induction of metabolic dysfunction to understand pathophysiological changes related to obesity, in humans this condition is only observed in 2-4% of the population (Liu et al., 2013). Hence, using WD in WT mice is preferred in the current study to mimic the commonly observed clinical conditions.

Previous studies have demonstrated that WD for 6-8 weeks can induce metabolic alterations and physiological changes in mice (Hintze et al., 2018). Increased total body weight, liver/body weight ratio, elevated lipid profile, such as cholesterol or HDL, and liver or heart fat accumulation can be results of this intervention. Thus, WD in WT diet mice can induce significant changes after certain time frame. When these mice are exposed to stress or cardiometabolic interventions such as ischemic stroke, the long-term outcome is significantly worse than the ND groups. Detailed mechanisms of stroke-WD are discussed in the following chapters. However, the early response to stress, trauma or especially ischemic stroke within hours is not known.

1.6. IgA production and Peyer's patches

Immunoglobulin A (IgA) is the most abundant mucosal antibody that plays a critical role in protecting the mucosal tissues from infections by preventing the attachment of pathogens to mucosal surfaces. IgA is produced by plasma cells, which are a type of white blood cell that produces antibodies. B cells are activated by antigens, which are substances that can trigger an immune response (HuusPetersen and Finlay, 2021).

Once activated, in the case of IgA, plasma cells secrete IgA into the mucosal secretions, such as saliva, tears, and intestinal secretions. IgA is then transported across the epithelial layer and into the lumen of the mucosal surface, where it can bind to and neutralize pathogens (HuusPetersen and Finlay, 2021).

The production and secretion of IgA is regulated by a number of factors, including the presence of antigens and the activation of immune effector cells. Peyer's patches (PP), which are clusters of lymphoid tissue found in the small intestine, play an important role

in this process by inducing germinal center responses and initiating immune responses against pathogens (Hand and Reboldi, 2021). PP are part of the gut-associated lymphoid tissue (GALT), which also includes isolated lymphoid follicles (ILFs) (Lycke and Bemark, 2012).

IgA production can be modulated in both T cell-dependent and T cell-independent manners in PPs. (Reboldi and Cyster, 2016). T cell-dependent IgA production involves the activation of B cells by T cells. This process leads to the formation of germinal centers (GC) within PP, where B cells proliferate and differentiate into antibody-producing cells. T cell-independent IgA production, on the other hand, can be induced by the stimulation of B cells with certain molecules, such as BAFF and APRIL, or their stimulation with Toll-like receptor (TLR) ligands (Hand and Reboldi, 2021).

Secretory IgA (SIgA) is the major immunoglobulin isotype in the intestinal mucosa. The majority of plasma cells producing IgA migrate from the PP via mesenteric lymph nodes (mLN) and later on through blood stream, ending in lamina propria (LP) of small intestines. SIgA protects against the adhesion of pathogens and their penetration into the intestinal barrier. The commensal microbiota, which are the microorganisms that live in the gut, are known to contribute to IgA production (Lycke and Bemark, 2012). Moreover, SIgA regulates gut microbiota composition and provides intestinal homeostasis (LiJin and Chen, 2020).

Research has shown that dietary antigens can induce GC responses in PPs and lead to the production of antigen-specific IgA (Hand and Reboldi, 2021). In one study, mice were maintained on an elemental diet that did not contain any large immunogenic molecules. The researchers found that dietary antigens contributed to IgA production in PPs through the induction of follicular helper T cells and GC B cells (Hara et al., 2019).

The role of dietary antigens in PP responses was further confirmed by adding bovine serum albumin (BSA), a protein found in cow's milk, to the elemental diet. The addition of BSA led to an increase in germinal center responses and IgA production (Hara et al., 2019). In addition to dietary antigens, the mononuclear phagocyte system (MPS) within PPs also plays a critical role in handling pathogens and initiating immune responses. The MPS includes dendritic cells and macrophages, which are types of white blood cells that

engulf and destroy pathogens. These cells are enriched in the subepithelial dome (SED) of PPs, where they interact with M cells, specialized epithelial cells that transport antigens from the gut lumen into PPs (Komban et al., 2019). Once antigens have been transported into PPs by M cells, they are taken up by dendritic cells and macrophages. These cells then present the antigens to immune effector cells, such as T and B cells, to initiate an immune response. This process leads to the activation of B cells and the formation of GC within PPs (Victora and Nussenzweig, 2022). Among other cell types, neutrophils also constitute about 1-3% of PPs, with macrophages. Yet, in lamina propria, where the plasma cells (PC) reside, previous studies have shown a greater number of neutrophils compared to PPs. Neutrophils in the LP and gut wall increase in number in response to inflammatory conditions, infection and inflammation. Hence, neutrophils might interact with other cells, especially PC in the same compartment.

In conclusion, PPs play a crucial role in the generation of PC precursors that will secrete IgA and protect mucosal barriers. Dietary antigens, commensal bacteria and the mononuclear phagocyte system within PPs both contribute to this process by inducing GC responses and initiating immune responses against pathogens. In LP, different cells and especially neutrophils may play a role in modulation of PC IgA secretion in different disease conditions, e.g. stroke.

1.7. Neutrophil and further immune cell invasion

In the context of stroke, neutrophils are recruited to the brain within hours of the onset of ischemia and they are the first immune cells to invade central nervous system after stroke (Cai et al., 2020). Neutrophils release pro-inflammatory cytokines, ROS, and proteases, which can damage brain tissue and exacerbate the inflammatory response. The invasion mechanisms of neutrophils into the brain after stroke are complex and involve a range of cellular and molecular interactions (Jickling et al., 2015).

The invasion process of neutrophils begins with the activation of endothelial cells, which line the blood vessels in the brain. Endothelial cells express adhesion molecules, such as intercellular adhesion molecule-1 (ICAM-1) and vascular cell adhesion molecule-1

(VCAM-1), which interact with integrins on the surface of neutrophils (Jickling et al., 2015). This interaction leads to the rolling and adhesion of neutrophils to the endothelial cells.

Once neutrophils have adhered to the endothelial cells, they undergo a process called diapedesis, which involves the migration of neutrophils across the endothelial cell layer and into the brain parenchyma. This process is facilitated by the expression of chemokines, such as CXCL1 and CXCL2, which are produced by endothelial cells, microglia and astrocytes in response to ischemia (Lin et al., 2023). Chemokines bind to receptors on the surface of neutrophils, which triggers the activation of intracellular signaling pathways that promote neutrophil migration. Once neutrophils have entered the brain parenchyma, they interact with other immune cells, including microglia and T cells (Zhang et al., 2021). Microglia are resident immune cells in the brain that play a critical role in the inflammatory response to stroke. They are activated by pro-inflammatory cytokines and chemokines, which are released by neutrophils and other immune cells. Activated microglia produce a range of pro-inflammatory cytokines, such as interleukin-1β (IL-1β) and tumor necrosis factor-α (TNF-α), which can exacerbate the inflammatory response and contribute to stroke pathophysiology by causing more immune cell activation (Lin et al., 2023).

T cells are another type of immune cell that infiltrate the brain after stroke. They are recruited to the brain by chemokines, such as CXCL10, which are produced by astrocytes and microglia. T cells play a critical role in the adaptive immune response and are thought to contribute to stroke pathophysiology by releasing pro-inflammatory cytokines and by interacting with other immune cells in the brain. CD4+ T cells are one of the main types of T cells that infiltrate the brain after stroke (Zhang et al., 2021). They are responsible for coordinating the immune response by recognizing antigens that are presented on the surface of antigen-presenting cells, such as dendritic cells and macrophages. Once activated, CD4+ T cells produce cytokines, which stimulate the proliferation and activation of other immune cells, such as B cells and CD8+ T cells. CD4+ T cells are also involved in the development of immunological memory. CD8+ T cells are another type of T cell that infiltrate the brain after stroke. They are responsible for killing targeted cells by recognizing antigens that are presented on the surface of infected cells in the context of major histocompatibility complex (MHC) class I molecules. Once activated, CD8+ T

cells release cytotoxic granules, which contain perforin and granzymes, that induce apoptosis in the target cells. Regulatory T cells (Tregs) are another type of T cell that infiltrate the brain after stroke. Tregs are responsible for suppressing the immune response and maintaining immune homeostasis. They do this by recognizing self-antigens and inhibiting the activation of other immune cells. Tregs are critical for preventing autoimmune diseases and for maintaining tolerance to self-antigens. Th17 cells are another type of CD4+ T cell that infiltrate the brain after stroke. Th17 cells are responsible for producing interleukin-17 (IL-17), which is a pro-inflammatory cytokine that is involved in the recruitment of neutrophils and other immune cells to the site of infection or inflammation. Finally, memory T cells are a type of T cell that infiltrate the brain after stroke and are responsible for maintaining immunological memory. Memory T cells are generated during an immune response and are long-lived. They are able to rapidly respond to a subsequent exposure to the same antigen and are critical for long-term protection against pathogens (Wang et al., 2023).

Furthermore, neutrophils can both suppress and activate T cell subsets in different conditions via differential regulation of certain cytokines. When in close contact, neutrophils can inhibit T cell activation via integrins and also H2O2 release. Neutrophils can also increase arginase-1 production to attenuate T cell activation under certain conditions, such as in glioblastoma. On the other hand, neutrophils can activate T cells via release of MCP-1, CCL1, CCL2, CCL5 or CXCL10 in several disease models (Zhang et al., 2021). These cytokines have multiple effects on different subsets of T cells. For instance, MCP-1 can enhance immune response of CD8+ cells; IL-17 activates CD4+ T cells; whereas CXCL10 increases the effect of Th1 cells. In certain conditions, this cascade also includes Neutrophil Extracellular Traps (NET) released by neutrophils. NETs were shown to prime T cell activation in vitro via increasing their cytokine production and proliferation. Moreover, neutrophils can play a crucial role as antigen presenting cells (APC) to prime T cells via MHCII, CD80 and CD86. For example, neutrophils can secrete interferon-gamma (IFN-γ), which is a pro-inflammatory cytokine that is involved in the activation of CD8+ T cells. Neutrophils can also secrete TNF-α, which is a pro-inflammatory cytokine that is involved in the activation of CD4+ T cells (Wang et al., 2023).

In conclusion, neutrophils are a critical component of the innate immune response and are also involved in the regulation of the adaptive immune response after stroke. Recent studies have shown that neutrophils can secrete cytokines, such as IL-17, IFN-γ, and TNF-α, that induce T cell activation.

1.8. Neutrophil Activation

Neutrophils are key regulators as a part of innate immune system, via phagocytosing and killing invading pathogens or being activated after sterile tissue injury and they are recruited to the site of injury or infection within hours of the onset of ischemia. The activation of neutrophils is a complex process that involves the recognition of damage-associated molecular patterns (DAMPs) and the high mobility group box 1 (HMGB1) protein, as well as the interaction of neutrophil receptors with these molecules (Papayannopoulos, 2018). DAMPs are endogenous molecules that are released from damaged or dying cells. DAMPs can activate neutrophils by binding to pattern recognition receptors (PRRs) on the surface of neutrophils. The two main types of PRRs that are involved in the activation of neutrophils by DAMPs are Toll-like receptors (TLRs) and NOD-like receptors (NLRs). TLRs are a family of PRRs that are expressed on the surface of neutrophils and other immune cells (Pittman and Kubes, 2013). They recognize a wide range of DAMPs, including heat shock proteins, HMGB1, and DNA. NLRs recognize a wide range of DAMPs, including uric acid, ATP, and HMGB1. The binding of DAMPs to TLRs and NLRs on the surface of neutrophils triggers the activation of intracellular signaling pathways that promote neutrophil activation and migration. HMGB1 is a nuclear protein that is released from damaged or dying cells and is recognized by the immune system as a DAMP. HMGB1 can activate neutrophils by binding to several different receptors on the surface of neutrophils, including the receptor for advanced glycation end products (RAGE), TLR2, and TLR4. RAGE is a receptor that is expressed on the surface of neutrophils and other immune cells. It recognizes a wide range of ligands, including HMGB1, and is involved in the activation of neutrophils and other immune cells. In conclusion, the activation of neutrophils is a complex process that involves the recognition of DAMPs and the HMGB1 protein, as well as the interaction of

neutrophil receptors with these molecules (Papayannopoulos, 2018). Understanding the mechanisms of neutrophil activation is critical for the development of new treatments for conditions that involve neutrophil infiltration, such as stroke and other inflammatory diseases. These diseases affect patients with different morbidities. Hyperlipidemia is one of the most common comorbidities in stroke patients, which was shown to be associated with worse outcome. In these patients, higher amounts of lipids might regulate neutrophils, which might in turn cause worse prognosis. Hence, it is crucial to understand neutrophil and adipose tissue/lipid interactions.

1.9. Neutrophil modulation by lipids

Recent studies have shown that neutrophils can interact with adipose tissue, which is a complex endocrine organ that plays a critical role in metabolism and inflammation. The interaction of neutrophils with adipose tissue is a complex process that involves the recognition of adipose tissue-derived molecules and the interaction of neutrophil receptors with these molecules. Adipose tissue is a complex endocrine organ that is composed of adipocytes, immune cells, and other cell types. Adipose tissue is involved in the regulation of metabolism and inflammation and is a major source of cytokines and other signaling molecules. Recent studies have shown that adipose tissue can interact with neutrophils, which are recruited to adipose tissue during obesity and other metabolic disorders. The interaction of neutrophils with adipose tissue is thought to contribute to the pathogenesis of obesity and other metabolic disorders. Neutrophils can release a range of pro-inflammatory cytokines, reactive oxygen species, and proteases, which can damage adipose tissue and exacerbate the inflammatory response (Watanabe et al., 2019). The activation of neutrophils in adipose tissue is also thought to contribute to the recruitment of other immune cells, including macrophages and T cells, to adipose tissue.

Adipose tissue-derived molecules that have been shown to interact with neutrophils include adipokines, such as adiponectin and leptin, and free fatty acids (FFAs). Adiponectin is an adipokine that is produced by adipocytes and is involved in the regulation of metabolism and inflammation. Adiponectin has been shown to have anti-inflammatory effects and is thought to play a protective role in the development of

metabolic disorders. Recent studies have shown that adiponectin can interact with neutrophils and inhibit their activation and migration. The interaction of adiponectin with neutrophils is thought to involve the adiponectin receptor 1 (AdipoR1) and the adiponectin receptor 2 (AdipoR2), which are expressed on the surface of neutrophils. Leptin is another adipokine that is produced by adipocytes and is involved in the regulation of metabolism and inflammation. Leptin has been shown to have pro-inflammatory effects and is thought to contribute to the development of metabolic disorders. Recent studies have shown that leptin can interact with neutrophils and activate their migration and phagocytic activity. The interaction of leptin with neutrophils is thought to involve the leptin receptor (ObR), which is expressed on the surface of neutrophils. FFAs are another class of adipose tissue-derived molecules that have been shown to interact with neutrophils. FFAs are released from adipocytes during lipolysis and are involved in the regulation of metabolism and inflammation. Recent studies have shown that FFAs can activate neutrophils and promote their migration and phagocytic activity. The interaction of FFAs with neutrophils is thought to involve several different receptors, including TLR4, G protein-coupled receptor 40 (GPR40), and G protein-coupled receptor 120 (GPR120) (BlaszczakJalilvand and Hsueh, 2021).

In addition to direct adipose tissue neutrophil interactions, WD fed mice show different circulating neutrophil characteristics in comparison to normal chow fed mice. WD induced hypercholesterolemia, which caused more neutrophils to circulate in blood. These neutrophils were correlated with atherosclerotic plaque formation, in which neutrophils invaded the newly plaque formation and recruited other cell types. Furthermore, in hypercholesterolemic mice, higher serum TNF and IL17 levels were measured, which also resulted in more G-CSF secretion, and neutrophil recruitment. These results suggest higher neutrophil production and recruitment in hyperlipidemic mice (Drechsler et al., 2010).

In the context of neutrophil regulation by lipids in stroke pathophysiology, several preclinical studies revealed crucial fundamental mechanisms. Hyperlipidemic apolipoprotein-E deficient (ApoE−/−) mice have been found to exhibit significantly more severe cerebral ischemic injury compared to normolipidemic wildtype mice. This increased injury was associated with elevated granulocyte counts in both the spleen and bloodstream (Herz et al., 2014). Moreover, the study has shown that the exacerbation of

ischemic brain injury in ApoE−/− mice can be mitigated by depleting polymorphonuclear neutrophils (PMN) using Ly6G antibodies, inhibiting PMN entry into the brain via pharmacological blockade of the CXC motif receptor-2 (CXCR2), or introducing a CXCR2 blocking antibody (Herz et al., 2015). These findings suggest that PMN are accountable for the worsening of brain injury in hyperlipidemic conditions being a major stroke risk factor. However, the precise molecular mechanisms through which invading PMN impede brain remodeling or the time course of this mechanism remain unelucidated.

PMN are known to abundantly generate and release pro-inflammatory cytokines after induction of ischemic stroke, which promote the opening of the blood-brain barrier (BBB), release of reactive oxygen species that induce structural damage to brain extracellular matrix (ECM) proteins, and hydrolytic enzymes, such as elastase, that degrade ECM proteins and proteoglycans (Huang et al., 2020). In hyperlipidemic conditions, there is an increase in BBB permeability, which is further exacerbated by the upregulation of calpain1/2 and MMP2/9. In addition to BBB permeability, brain edema also increases in hyperlipidemic conditions, being a further risk for patients with stroke. The Rho GTPase RhoA also plays a crucial role in maintaining tight junctions in the BBB, that is disturbed after stroke, which is worsened in hyperlipidemic conditions (ElAli et al., 2011). Furthermore, in hyperlipidemic mice, CXCR2 inhibition has been shown to offer protection, in contrast to no difference with CXCR2 inhibition in normolipidemic mice. As hyperlipidemic mice show higher levels of CXCL1-2 expression in the arteries, this might be the reason of brain protection with CXCR2 inhibition. Additionally, there is an increase in NO synthase and NADPH oxidase 2 in hyperlipidemic mice, which could potentially influence ICAM and VCAM expression in vessels. Even though vessel density is not affected, interestingly, ICAM expression was highly upregulated in ApoE-/- stroke mice compared to normolipidemic mice after 72h of stroke induction, while VCAM was moderately upregulated. Yet, after 24 h of stroke, hypercholesterolemic mice showed higher endothelial activation (ICAM-1), with or without ApoE knockout (Herz et al., 2015, Herz et al., 2014). In addition to endothelial activation and neutrophil migration, neutrophil extracellular trap release also plays a crucial role in stroke pathophysiology. Studies with ischemic stroke thrombi characterization in humans revealed a relation with citH3+ regions (NET formation) and stroke severity (Laridan et al., 2017). Furthermore, studies with NET inhibition or degradation revealed neuroprotection in preclinical

ischemic stroke models (Kang et al., 2020, Rolfes et al., 2021, Denorme et al., 2022). Furthermore, hyperlipidemia also attenuates vascular remodeling via decreased pericyte coverage and activation, induces more brain hemorrhage associated pro-inflammatory responses related to worse prognosis, even in cases where cerebroprotective medications are given (Yin et al., 2023, Zechariah et al., 2013). Hence, inhibiting NET release and modulating hyperlipidemia induces changes in immune cells might have beneficial effects in vascular and pericyte protection especially in hyperlipidemic mice (Zechariah et al., 2013). NET inhibition was shown to increase microvascular circulation, less damage to neurons and result in better outcome (Denorme et al., 2022). Yet, the impact of NETs outside central nervous system is not known.

In conclusion, the interaction of neutrophils with adipose tissue and regulation of neutrophil activation via hyperlipidemic conditions are complex processes that involve the recognition of adipose tissue-derived molecules, he interaction of neutrophil receptors with these molecules, endothelial activation and higher neutrophil migration with ROS-NET release. Understanding the mechanisms of neutrophil-adipose tissue interactions is critical for the pathophysiology of ischemic stroke in patients with obesity or hyperlipidemia. The inhibition of neutrophil activation in adipose tissue is a promising therapeutic strategy that has shown efficacy in animal models of obesity and other metabolic disorders. In stroke, inhibiting priming of neutrophils by adipose tissue might be target to stop overshooting of immune responses after cerebral ischemia.

2.Aim of the study

Stroke is the second most common reason of mortality and morbidity worldwide. Stroke patients suffer from infections, gastrointestinal bleeding, dysphagia and many other complications. Yet, in the last decades, there is no new approved targeted therapy to treat stroke or related complications. Infections or immune system disturbances account for more than 30% of the complications after stroke, hence, our study first aimed at understanding the regulation of IgA, the most abundant mucosal antibody and defense mechanism against infections. Another contributor to immune system disturbances after stroke is the neutrophil activation, in which the proinflammatory neutrophils are detrimental to brain recovery. The regulation of this neutrophil hyperactivation might be regulated via comorbidities of stroke patients. Hence, the second part of the current study aimed to understand the impact of Western Diet on early neutrophil activation and the formation of NETs, specifically within 3hours (within stroke treatment therapeutic window of 4,5 hours after symptom onset).

3. Materials and Methods

3.1. Materials

3.1.1 Devices and Equipment

iMARK Microplate Absorbance Reader	BIORAD (Germany)
Carl Zeiss OPMI surgical microscope	Carl Zeiss (Germany)
Laser Doppler Flow reader	Moor Instruments (UK)
Feedback-controlled heating system	Harvard Apparatus, Holliston (USA)
Centrifuge 5430R	Eppendorf, Hamburg (Germany)
Centrifuge 5810R	Eppendorf, Hamburg (Germany)
MacsQuant Analyzer 16	Miltenyi, Bergisch Gladbach (Germany)
Automated Cell counter	Nexcelom Bioscience (USA)
ADVIA® 2400	Siemens, Erlangen (Germany)
Waterbath	Sigma-Aldrich, Missouri (USA)
Vortex Genie 2	Scientific Industries, Bohemia (USA)
Pipette boy – Pipetus	Hirschmann Laborgeräte (Germany)
Pipette 2.5, 10, 20, 200, 1000 µL	Eppendorf, Hamburg (Germany)
Round handled suture tying forceps (11026-10)	Fine Science Tools (Germany)
Dumont #7 Forceps (11297-00)	Fine Science Tools (Germany)
Narrow pattern forceps (11002-12)	Fine Science Tools (Germany)
Halsted mosquito hemostats (13008-12)	Fine Science Tools (Germany)
Fine scissors – sharp (14060-09)	Fine Science Tools (Germany)
Fine scissors – sharp long (14060-11)	Fine Science Tools (Germany)
Spring scissors- 8mm cutting 0.2mm tip (15024-10)	Fine Science Tools (Germany)
Vannas spring scissors -3 mm cutting curved (15000-10)	Fine Science Tools (Germany)

Vannus spring scissors – 3 mm cutting straight (15000-00)	Fine Science Tools (Germany)
Semken forceps (11008-13)	Fine Science Tools (Germany)
2 mm silicon-coated filament (Cat. 702234PK5Re)	Doccol (USA)
Silk suture 5-0 (Cat. K890H), 7-0 (Cat. EH7464G)	Ethicon, Norderstedt (Germany)
Nylon suture 6-0 (Cat. 667H)	Ethicon, Norderstedt (Germany)

3.1.2 Consumables

10 mL pipette	Greiner Bio One (Austria)
Cell counting chamber	Nexcelom Bioscience, Massachusetts (USA)
15 mL; 50 mL Falcon tube	Greiner Bio One (Austria)
EDTA-tube	Sarstedt, Nümbrecht (Germany)
MACS smart strainer 70 um	Miltenyi Biotec (Germany)
Sysmex celltrics 30 um	pluriSelect, Leipzig (Germany)
Discardit II syringe 2 mL	BD, Heidelberg (Germany)
Injekft F Duo, 25 G Syringe 1 mL	B.Braun, Melsungen (Germany)
5 mL round bottom polystyrene tube	Fisher Scientific, Massachusetts (USA)
Human IgA uncoated ELISA kit (Cat. 88-50600-22)	Thermo Fisher Scientific (USA)
Percoll	Sigma-Aldrich, Missouri (USA)
CD19 Alexa Fluor 594	Biolegend (USA)
CD3 Alexa Fluor 647	Biolegend (USA)
LEGENDplex™ Mouse Proinflammatory Chemokine Panel (13-plex) with V-bottom Plate (Cat. 740622)	Biolegend (USA)

3.1.3 Chemicals and buffers

MACS Quant Running Buffer	Miltenyi, Bergisch Gladbach (Germany)
RBC-lysis Buffer	1 L: 150 mM NH4CL (MW: 53,49 g/mol; 8.02 g), 10 mM KHCO3 (MW: 100.12 g/mol; 1g), 0.1 mM EDTA (200 uL of 0.5 M EDTA), dH2O, pH 7.2 (adjust with KOH or HCl) stored at 4 °C for long-term use
PBS	1 L dH2O + 0,2 g KCl + 0,27 g KH2PO4 + 1,42 g Na2HPO4 + 8 g NaCl pH 7.2 (adjusted with HCl or NaOH)
Permeabilization buffer (LSFM)	20%DMSO 1%Triton X100 2.3mg/100ml Glycine in PBS
Blocking buffer (LSFM)	0.1%Saponin 0.1%TritonX100 0.02%Na-azide 6% rat serum in PBS
Dehydration buffer (LSFM)	30%, 60%, 80% EtOH solutions prepared in ddH2O and 100% EtOH
Ethyl cinnamate (ECi, Cat. 112372)	Sigma-Aldrich, Missouri (USA)

3.2. Methods

3.2.1 Human Samples

The ethical approval for the use of healthy and stroke patients' plasma was granted as per the institutional ethics board committee of the University Hospital Essen (Study number: 18-8408-BO and 23-11200-BO). Blood samples from stroke patients were taken at the University Hospital Essen Stroke Unit within seven days after symptom onset. Samples were centrifuged at 900 g for 20 min, followed by a second centrifuge at 2000 g for 15 min to separate plasma. Aliquots from plasma were stored at -80°C until further analysis.

3.2.2 Plasma IgA Measurement

Plasma samples were thawed and used to measure plasma IgA levels using IgA human uncoated ELISA kit as described by the manufacturer. The ELISA plates were coated overnight with anti-IgA antibody overnight at 4°C. Afterwards, the wells were washed in total 4-times with washing buffer and blocked with blocking solution supplied with the kit for 2 hours. This step and following steps were done on a plate shaker in 300rpm, unless otherwise mentioned. During blocking, samples dilutions were prepared, even though the kit recommendation was 1:10000 dilution, the optimisation was found to be 1:20000 dilution in kit solution. Afterwards, the plate was washed 4-times with washing buffer and samples were added for incubation during 2 hours. Wells were washed 4-times with washing buffer and detection antibody (coupled with HRP) was added. Afterwards, substrate was added to wells and incubated without shaking. The reaction was stopped after 30min and measured in ELISA plate reader.

3.2.3 Plasma NETs quantification

NETs quantification was performed on EDTA plasma using a citrullinated histone H3 associated with DNA (Sun et al., 2021). Anti-histone H3 antibody (5 µg/ml; ab5103, Abcam) or neutrophil elastase antibody (5 µg/ml; ab68672, Abcam) were coated overnight at 4°C onto 96-well plates followed by 5% BSA blocking for 2 h. Wells were three times washed with 300 µl washing buffer followed by the addition of 50 µl plasma and 80 µl incubation buffer (including peroxidase-labeled anti-DNA antibody) for 2 hours at 300 rpm (Cell Death ELISAPLUS, Cat. 11774425001, Roche). Then, the wells were washed three times with 300 µl washing buffer and 100 µl peroxidase substrate was added to the wells for 30 min in the dark. Afterwards, 100 µl ABTS peroxidase stop solution was added to the wells, and absorbance was measured at 405 nm and was subtracted by absorbance at 490 nm (Abs 405 nm-Abs 490 nm). The absorbance values were considered in direct proportion to the amounts of soluble NETs and were presented as a relative increase to control.

3.2.4 Animals

All animal experiments were performed in accordance with ethical guidelines and were approved by the local authorities (G1713/18, G1719/19) of Landesamt für Natur, Umwelt und Verbraucherschutz Nordrhein-Westfalen, Recklinghausen, Germany). Male C57BL/6JHsd wild-type mice were obtained from Envigo (Netherlands). The mice were randomly divided into two groups: sham and tMCAO surgery (stroke). Western diet (Cat No: E15721-347, Ssnif) was provided to Western diet (WD) group beginning from 5 weeks of age for 6 weeks. All animals were operated between the age of 8-10 weeks of age. The animals had ad libitum access to food and water. Animals were kept in a regular inverse 12 h: 12 h light/dark cycle in groups of 5 animals/cage. All experiments were reported according to ARRIVE guidelines (Kilkenny et al., 2012).

3.2.5 Mouse model of stroke

Brain injury was induced by transient middle cerebral artery occlusion (tMCAO) in C57BL/6JHsd mice (aged 8-10 weeks) anesthetized with 1% isoflurane in 100% oxygen. Mice were injected with the analgesic buprenorphine (0.1 mg/kg body weight, s.c.) 30 min before surgery. An eye ointment (Bepanthen) was applied to avoid harm to the mouse eyes during the surgical procedure.

A small incision was made between the ear and eye to expose the temporal bone, and a laser Doppler flow probe was attached to the skull above the core of the middle cerebral artery (MCA) territory. The mice were then placed in the supine position on a feedback-controlled heat pad, and the midline neck region was exposed with a small incision. The common carotid artery (CCA) and left external carotid arteries were identified and ligated. A 2 mm silicon-coated filament (Cat. 702234PK5Re; Doccol) was inserted into the internal carotid artery to occlude the MCA. Brain ischemia was validated by a stable reduction in blood flow to ≤ 20% of baseline that was observed on the laser Doppler flow device

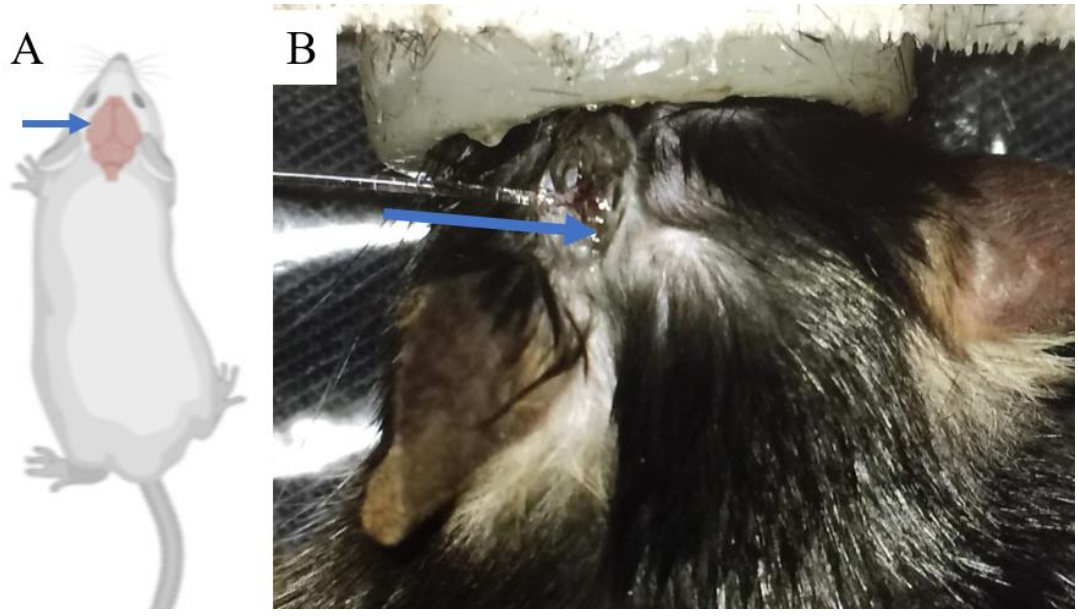

Figure 2: Insertion of LDF to temporal bone. A, Sketch showing the incision area in mouse head. B, Picture from surgical intervention showing LDF probe and opened skull.

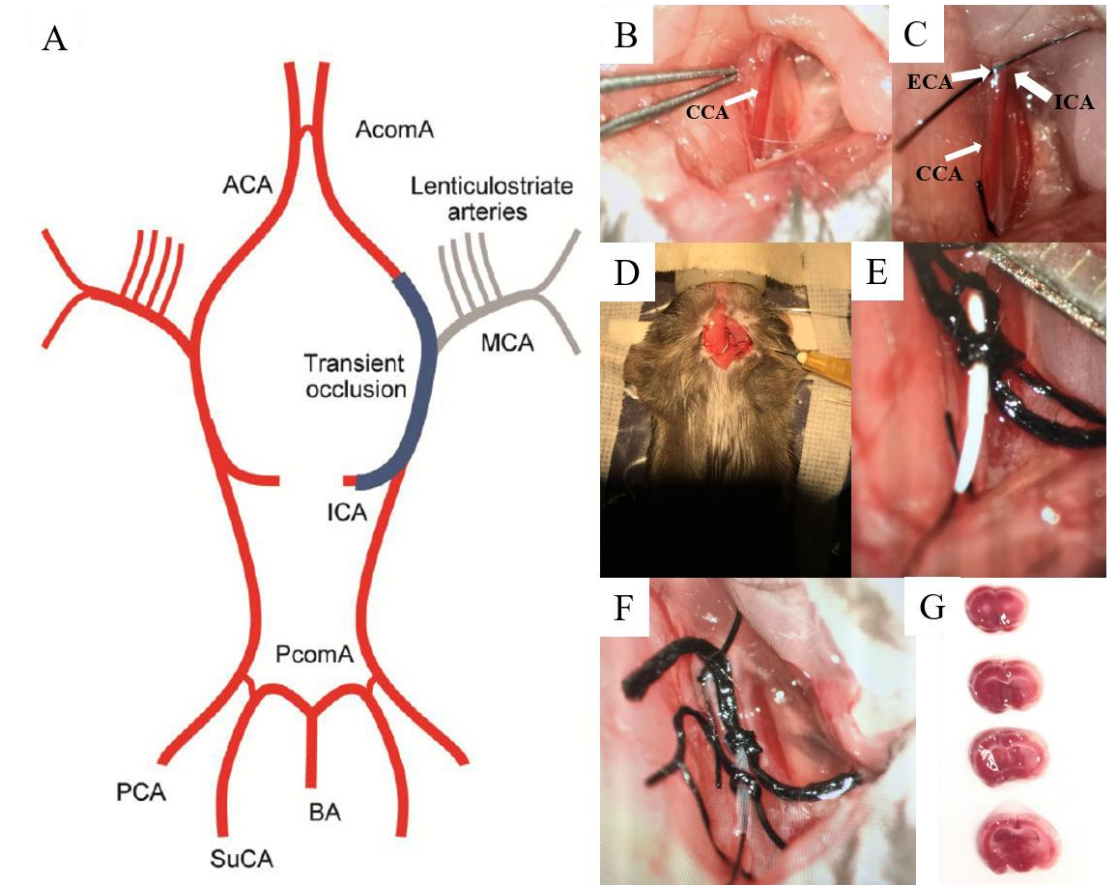

Figure 3: Scheme of tMCAO model. A, Schematic diagram showing Circle of Willis supplying blood to brain and inserted filament in blue to occlude middle cerebral artery. B, C, D, E, F, Representative pictures from surgical microscope showing tMCAO surgery steps. B, Common carotid artery (CCA) is dissected from carotid sheath. C, After suturing CCA, external (ECA) and internal carotid arteries (ICA) are dissected, ECA is sutured to avoid bleeding. D, Zoomed-out photo showing the incision area, inserted filament to CCA. E, The monofilament is inserted into CCA via a small incision to CCA, afterwards (F) advanced until occluding MCA. G, The tMCAO surgery results in consistent replicable infarcts in cortical and striatal brain regions after 60 min of occlusion.

After 60 min of occlusion, the filament was removed for the reestablishment of blood flow. Mice were then injected with the anti-inflammatory drug carprofen (4-5 mg/kg body weight, s.c.), wounds were carefully sutured, and the mice were returned to their cages with free access to food and water. Sham-operated mice underwent the same surgical protocol, except that the filament was inserted into the CCA and immediately removed. The exclusion criteria for experimental mice were as follows: inadequate ischemia

(reduction of blood flow does not reach ≤ 20% of baseline threshold), weight loss >20% of baseline body weight during the study, and spontaneous animal death.

3.2.6 Optical clearing of Peyer's patches

Mice were sacrificed and small intestines were dissected and placed in Petri dishes containing cold PBS. The intestinal tissue was then divided into four sections and cleaned from intestinal contents using cold PBS. About one cm of intestinal tissue containing PP was cut and further cleaned to remove food contents. Further, samples were embedded in 1.5% low melting agarose using plastic tissue molds, and samples were placed on ice. After 20 minutes, samples were carefully removed from the molds and extra solidified agarose was trimmed with a sharp surgical knife. Samples were then fixed with 4% PFA in PBS overnight at 4°C. The next day, samples were treated with a series of ethanol (EtOH) solutions starting from 30% and 60%, 80%, and 2 times 100%. Samples were kept in each solution for 12 h on an orbital shaker (50 rpm at 8°C) before a change to the higher percentage solution. At last, samples were treated with ethyl cinnamate (ECI, Cat. 112372-100G, Sigma) to match the refractive index and light-sheet fluorescence microscopy (LSFM) was performed.

3.2.7 Light Sheet Fluorescence Microscopy for Peyer's patch volume analysis

The cleared samples of PP were imaged using LSFM (UltraMicroscope BLAZE and UltraMicroscope II, Miltenyi Germany). The microscope systems employ the software ImSpector (LaVision BioTec, Germany). Samples were placed in the chamber filled with 100% ECI with the help of a steel holder. The autofluorescence of the sample was measured at 488 nm using an Optically Pumped Semiconductor Laser (OPSL; 50 mW) that was filtered through a 525/50 nm bandpass filter. The light-sheet width has been set to 30% and the numerical aperture was set to 0.05. These settings correspond to a light-sheet thickness of 15 µm. The images were acquired with a zoom factor of 3.2X with an interval of 5 µm. For volume analysis, the images were processed using Imaris software version 9.5.1 (Bitplane, Switzerland). The Imaris File Converter was used to convert

images. Software-own Gaussian and smoothing filters were used. The quantification of the volumes was performed with Imaris surface function and volumes were calculated. For this, every 25 µm area measurement of PP was performed in the autofluorescence channel.

3.2.8 Whole-mount staining of PP and LSFM analysis

Mice were sacrificed and small intestines were dissected and placed in Petri dishes containing cold PBS. Intestinal tissue proximal to the cecum was cut into three pieces; duodenum, jejunum, and ileum, respectively. Intestinal tissue, 5 mm proximal and distal to each PP, was cut and transferred to 4% PFA in separate 2 ml Eppendorf tubes and incubated for 2 h at RT. Samples were washed in PBS for 2 h and cleaned from intestinal contents and fat using PBS. Cleaned PP were transferred to 1 ml permeabilization buffer and incubated overnight on an orbital shaker (60 rpm). The following day, samples were transferred to a blocking buffer including 6% rat serum and incubated overnight on an orbital shaker (60 rpm) at 4°C. Further, samples were transferred into 2 ml Eppendorf tubes with blocking buffer containing 3% rat serum, and 1 µg purified anti-mouse CD16/32 antibody (BioLegend) for 30 minutes. Then, anti-CD19 Alexa Fluor 594 and anti-CD3 Alexa Fluor 647 (BioLegend) antibodies were added, and samples were incubated overnight at 4°C. Samples were transferred to new glass vials and washed with PBS for 1 h and then with freshly added PBS overnight with continuous shaking (60 rpm). The day after, samples were embedded in 1.5% low-gelling agarose using plastic tissue molds and put on ice for 20 minutes. Samples were then carefully removed from the molds and extra solidified agarose was trimmed with a sharp surgical knife. Samples in solidified agarose were transferred to fresh brown vials containing 2 ml 30% EtOH, followed by serial treatment of 60%, 80%, and 100% EtOH for 1 hour in each solution and then 100% EtOH incubation overnight. All steps were performed with continuous shaking of samples (60 rpm). Samples were finally transferred to ECI in fresh glass vials and imaged after 3 h.

The cleared and stained PP samples were imaged by LSFM (Ultramicroscope BLAZE, Miltenyi Biotech, Germany). Samples were placed in the chamber filled with 100% ECI solution with the help of a steel holder. B cells stained with anti-CD19 Alexa Fluor 594

were illuminated with a 595/20 nm OPSL and were detected by a 650/50 nm band pass filter. T cells stained with anti-CD3 Alexa Fluor 647 were measured at 630/30 nm using an OPSL and were detected by a 680/30 nm band pass filter. The light-sheet width has been set to 40% and the numerical aperture was set to 0.05. These settings correspond to a light-sheet thickness of 4 µm. The images were acquired with a zoom factor of 6.4 X with an interval of 5 µm. 3D images were prepared using Z-stacks in the software Imaris version 9.5.1 (Bitplane, Switzerland). The Imaris File Converter was used to convert the images.

3.2.9 Machine learning-based pipeline for B cell volume analysis of LSFM images

The respective analysis algorithms are written by Dr. Chen (ISAS Dortmund). Briefly, the volume of B cells and T cells was measured from the segmentation results of the corresponding channels of the 3D LSFM images. A human-in-the-loop deep learning-based segmentation method was employed to obtain the final segmentation results. The overall segmentation workflow was generalized from the iterative deep learning workflow in the Allen Cell and Structure Segmenter. During this process, human experts were only asked to manually annotate two image z-stacks for the initial training of the deep neural network models, and then only to perform curation and minor error correction, to minimize the human effort. After the initial training, the model was applied to all images to generate segmentations, including post-processing steps, such as binarization and removing small false-positive objects from the model prediction. The results were provided to human experts to review. Segmentations either with negligible/minor errors or with big errors but straightforward to fix were selected. After fixing the errors, the curated subset was used to further train the segmentation models, which would then be applied to all images again. Such a loop will terminate when all segmentations were of good quality. Two different models were developed for B cells and T cells, respectively.

It is worth mentioning that there is no absolute per-pixel ground truth for the segmentation due to the limited resolution and diffraction of light. In other words, human experts can only tell if the segmentation is reasonable or not, but cannot be certain on every individual

pixel if it belongs to B cells /T cells or not. For this reason, human curation (i.e. deciding if the preliminary segmentation is reasonable or not and making very minor corrections) is more useful and more efficient than human manual annotation of the images. It has been observed that the segmentation generated from the deep learning model was of better quality than human's direct annotation, especially in terms of 3D spatial consistency of the segmentation (e.g, a manually slice-by-slice annotated 3D ball-shaped object looks zig-zag from XZ or YZ side view, while the model's prediction is more consistent with a 3D ball-shaped). The models were able to learn useful knowledge from the noisy training data.

The images were down-sampled in XY dimensions by a ratio of 0.25. The neural network architecture was the enhanced 3D UNet, trained with a weighted sum of DICE loss and cross-entropy loss on a single NVIDIA A100 GPU. All details for model training and inference can be found at https://github.com/MMV-Lab/peyers_patch. The trained models are available at https://zenodo.org/record/6302990#. YhyocqvMI2x for reproducibility. For the final volume analysis, volumes in pixels obtained from volume analysis were converted to micrometer cubes, by multiplying with the voxel size of 0.975*0.975 at 5 µm intervals.

3.2.10 Immune cell isolation

Mice were deeply anesthetized with ketamine and xylazine (100 mg/kg/10 mg/kg, i.p.) and sacrificed afterwards. Blood was instantly collected via cardiac puncture and added to EDTA containing tubes. The mice were then perfused with phosphate-buffered saline (PBS), and gastrointestinal tract. spleen and BM were collected in 1.5 mL Eppendorf tubes chilled with ice containing PBS.

3.2.10.1. Single-cell preparations from PP and mLN

After taking out the gut of mice, the samples were transferred to cold boxes with ice. A light with an adjustable focus was prepared to focus on focal gut segments. Blue gloves were taken and under the light source, whole small intestinal tissue was scanned for PP. When a PP was found, that area was cut out without including neighboring intestinal tissue to avoid cell analysis from gut wall. After isolation, the number of PP per mouse

was noted. The cells from PP and mLN were harvested by cutting the tissues with several strokes of sharp scissors and passing them through 30 µm cell strainers. After washing with 10ml PBS two times, the samples were transferred to MACS buffer until counting. Single-cell suspensions were kept on ice until further use. The total cell counts per mouse were counted and analyzed as described below.

3.2.10.2. Single-cell preparations from blood

After opening thoracic cage and cutting diaphragm, the blood was collected by cardiac puncture to right ventricle with a 22-gauge needle and 1 mL syringe. Afterwards, blood was placed in EDTA tubes, and inverted several times to avoid clumping of the blood. Blood samples were centrifuged at 3000 g for 10 min at 14 °C and the supernatant plasma was collected for further analysis. Supernatant was collected in 500 µl Eppendorf tubes and centrifuged at 8000 g for the second time for 10min at 4°C, the supernatant was collected and stored in -80°C until further plasma analysis. For the isolation of blood cells, the amount of supernatant collected was added up with PBS and resuspended thoroughly. Blood samples (100 µL) were then placed in a 5 mL FACS tube and allowed to stand at room temperature for 10 min. For erythrocyte removal, prewarmed 2 mL of RBC lysis buffer was added to samples and vortexed. After at least 2 min of exposure time, 2.5 mL of PBS was added, and the blood samples were centrifuged at 1500 rpm for 5 min at 21 °C. The cell supernatant was removed, and the samples were washed again with 4 mL of PBS at 1100 rpm for 5 min at 21 °C. After removing the cell supernatant, a final wash was performed with 1 mL of MACS buffer and centrifuged at 1000 rpm for 5 min at 4 °C. The supernatant was discarded and 500 µL of MACS buffer was added. The cell suspension was then ready for the automated cell counter (Nexcelom Bioscience) without dilution. The single-cell suspensions were kept on ice until further use.

3.2.10.3. Single-cell preparations from spleen

Spleens were cut with scissors multiple times and grinded with the flat end of a 2ml syringe plunger, which was put on a 70µm pre-moistured with PBS on a 50ml Falcon tube. Spleen pieces were washed with 20ml PBS while smashing to filter the single cells through filter. Then the solutions were centrifuged at 1500 rpm for 5 min at 21 °C. The cell pellet was examined and the supernatant was carefully discarded. To remove the erythrocytes from the suspension, 1 mL of prewarmed at 37 °C RBC-Lysis buffer was first used to resuspend the cell pellet and followed by an addition of 4 mL of RBC-Lysis

buffer for 2 min. After sufficient reaction time, 20 mL of PBS was added and centrifuged again at 1500 rpm for 5 min at 21 °C. The supernatant was discarded again, the fat tissue was removed with a pipette, and 10 mL of PBS tubes were centrifuged at 1100 rpm for 6 min at 21 °C. After the final centrifugation, the supernatant was removed and the cell suspension was mixed in a final volume of 1 mL MACS buffer, placed on ice, and diluted in a separate 500µl Eppendorf tube 1:100 for automated cell counting. The single-cell suspensions were kept on ice until further use.

3.2.10.4. Single-cell preparations from bone marrow

Tibia was isolated through an incision a few millimeters above the knee joint, carefully freed from the muscle tissue, and knee joint was forced outwards to have the tibia free. The bones were placed on ice in 500 µL PBS until further treatment. After collection of all tibia samples from the included mice, both ends of the tibia were cut with sharp sterile scissors, and the BM was flushed at least twice with a 30-gauge fine needle and filtered through moistened 30 µm cell filters in a 15 mL Falcon tube while smashing with the flat end of a 1 mL syringe plunger. The collected cell suspension was centrifuged at 1500 rpm for 5 min at 21 °C. The supernatant was discarded, and the cell pellet was resuspended in 1 mL of RBC lysis buffer pre-warmed at 37 °C and treated for 2 min. After the addition of 5 mL of PBS, the cell suspension was centrifuged at 1500 rpm for 6 min at 21 °C, and the supernatant was discarded. After another wash with 1 mL MACS buffer at 1200 rpm for 6 min at 4 °C, the supernatant was discarded again, and the final suspension was made up with 1 mL MACS buffer. Diluted 1:20, the cells were ready for automated cell counting. The single-cell suspensions were kept on ice until further use.

3.2.11. Flow cytometry analysis

For each sample, 5×10^5 cells were stained with fluorochrome-conjugated antibodies against cell surface markers. The required amount was added to 5 mL FACS tubes, as indicated by the cell counter, and filled up to 100 µL with MACS buffer. If more than 100 µL was required to reach a cell count needed, most commonly in the case of blood samples, the required amount was centrifuged at 1500 rpm for 5 min at 4 °C and then resuspended in 100 µL. The suspensions were stained for 30 min with 10 µL of the

antibody according to the panel setup. The antibodies were then washed off with 1 mL of MACS buffer at 1500 rpm for 5 min at 4 °C, the supernatant was removed, and the residue was made up to 200 µL with cold MACS buffer for flow cytometry analysis. The measurements were performed using a MacsQuant Analyzer 16 (Miltenyi). The stop gate was set at 10.000 $CD45^+$ cells (leukocytes) to allow comparability between samples. Subsequently, all results were analyzed separately for each organ as a comparison medium using the FlowJo software (BD Biosciences).

3.2.12. Panel setup for neutrophil activation analysis

Antibody	**Clone**	**Catalog Nr.**	**Company**	**Function**
CD45	30-F11	103155	Biolegend	Used as leukocyte marker (excluding mature erythrocytes)
CD11b	M1/70	101206	Biolegend	Inflammatory response mediator via regulation of leukocyte adhesion and migration
Ly6G	1A8	127607	Biolegend	Neutrophil selection High Ly6G = mature Low Ly6g = immature
CD86	GL-1	105006	Biolegend	T cell activation and survival
Ly6C	HK1.4	128017	Biolegend	Monocyte gating High Ly6C = mature Low Ly6C = immature
CD68	FA-11	137010	Biolegend	Antigen presentation, co-stimulation
MHC II	M5/114.15.2	12-5321-81	Thermo Scientific	Antigen presentation; initiating immune response
CD182	SA045E1	149608	Biolegend	Chemokine receptor related to maturation of neutrophils
CD206	C068C2	141720	Biolegend	Functions in endocytosis and phagocytosis; role in immune homeostasis

CXCR4	L276F12	146511	Biolegend	Regulates migration towards sites of infections
CD62L	MEL-14	104407	Biolegend	Mediate rolling and adhesion to endothelial cells; regulate activation and migration into tissues
CD49d	R1-2	103619	Biolegend	Cell adhesion and signaling molecule
LFA-1	H155-78	141012	Biolegend	Firm arrest of leukocytes; emigration from blood to tissue
CD162	4RA10	12-1621-80	Thermo Scientific	High affinity counter receptor for cell adhesion molecules; role in trafficking during inflammation
CD284	SA15-21	145405	Biolegend	Pathogen recognition and activation of innate immunity

Table 1: List of antibodies included in neutrophil activation analysis

3.2.13. Quantification of brain infarct volumes

After removal of the blood, the mice were perfused with 20ml PBS, and organs (spleen, and bone marrow) were collected. Afterwards, the mice were perfused with 15ml 4% PFA then the brains were taken out and incubated in 4% PFA solution overnight. In the case of PP experimental setup, the mice organs were harvested without 4% PFA fixation and brains were directly put on dry ice with aluminum foil, changed to plastic boxes with respective labelling. Serial sucrose solutions of 15% and 30% were prepared and used for overnight incubation. The brains were then dried with thin tissue paper and quickly frozen on isopentane incubated on dry ice. The frozen brains were stored at -80 °C until further processing.

Samples of 20 µm thickness were taken from the brains at 500 µm intervals and stained with cresyl violet (Sigma, Cat. C5042). Thawed slides were first immersed in 100% ethanol for 15 minutes, followed by treatment with 70% and 50% ethanol for 1 minute each. The slides were then immersed twice in double-distilled water, with each immersion

lasting 2 and 1 min, respectively. In the next step, brain sections were incubated in prewarmed (65 °C) cresyl violet solution for 15 minutes. Subsequently, the sections were washed twice for 1 minute each in double-distilled water. Finally, the slides were washed twice for 1 minute each in 100% ethanol, mounted with 100 µl Roti-Histokitt, and covered with coverslips.

All sections were scanned at a resolution of 600dpi and then analyzed using ImageJ software. Using a conversion scale of 23.62 pixels per millimeter, the area of unstained infarct tissue was measured and integrated into the whole brain. Brain infarct volume was corrected for edema using the following formula: (ischemia area) = (direct lesion volume) - [(ipsilateral hemisphere) - (contralateral hemisphere)]. The resulting lesion volume for each hemisphere was expressed in mm^3.

3.2.14. Quantification of mouse plasma lipids and cytokines

Plasma samples (prepared as described above) were analyzed for total cholesterol levels using a bioanalyzer.

For the analysis of cytokines, manufacturer's instructions were followed (Cat. 740622, Biolegend), 12,5µl of mouse plasma was used for analysis. Briefly, samples were diluted with assay buffer and beads were vortexed. Beads were added to samples in the wells, covered with aluminum foil and shaken at room temperature for 2 hours at 800 rpm. After centrifugation, samples and controls were washed three times, followed by addition of detection antibodies. Afterwards, samples were shaken at room temperature for 1 hour at 800 rpm, followed by addition of SA-PE to be shaken for additional 30 min. After another round of washing, samples are detected at cytometer and analyzed in the manufacturer's software.

3.2.15. Statistical analysis

Statistical analysis of the data was performed using GraphPad Prism version 9.5.0. Data from stroke patients and healthy controls; naïve, sham and stroke mice within and across WD and ND were analyzed. Normality of the data distribution was checked within each

data set via Shapiro-Wilk normality test. Afterwards, two-sided Mann-Whitney U test was used to compare two groups. Statistical analysis among more than two groups was performed using either the One-Way ANOVA with Bonferroni`s multiple comparison post-hoc test (for normal distribution) or Kruskal-Wallis test (not-normal distribution). A Pearson-correlation was calculated between two parameters (citH3 and IgA), followed by linear regression analysis, shown by "r" value. A p-value of less than or equal to 0.05 was considered statistically significant.

3.2.16. Experimental Setup Outline

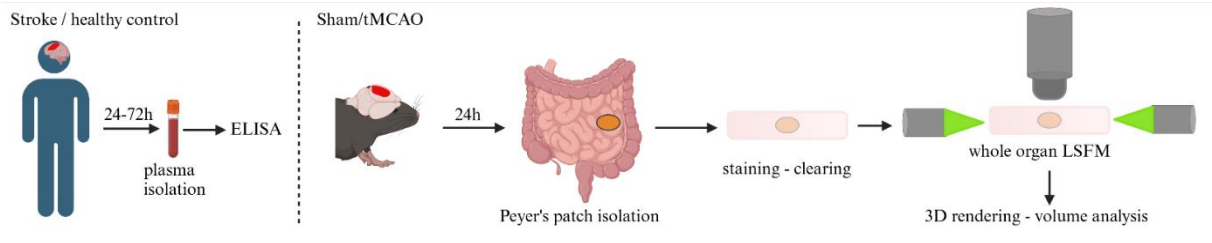

Figure 4: Experimental setup for ELISA measurements and LSFM analysis. Left: Blood samples were collected from stroke patients and healthy controls for analysis of plasma IgA and NETs using ELISA. Right: tMCAO was used to mimic stroke and IgA levels were measured using ELISA and PP volumes were analysed using LSFM.

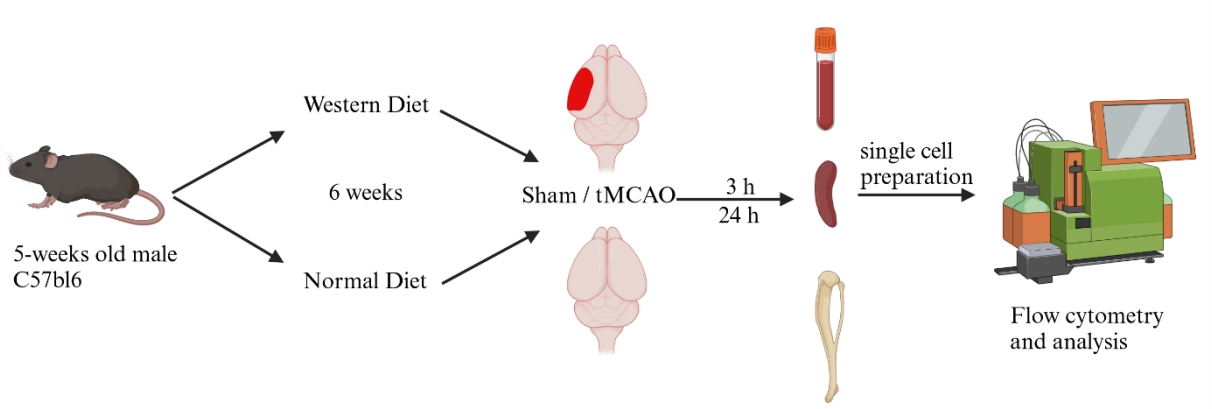

Figure 5: Experimental setup for Western Diet experiments. Mice were fed with Western Diet or Normal Diet and were subjected to tMCAO and sacrificed after 3 h or 24 h of reperfusion. Blood, spleen and tibial bone marrow were dissected to prepare single cell suspensions and analyzed via flow cytometry.

4. Results

4.1. Stroke patients show reduced amounts of plasma IgA

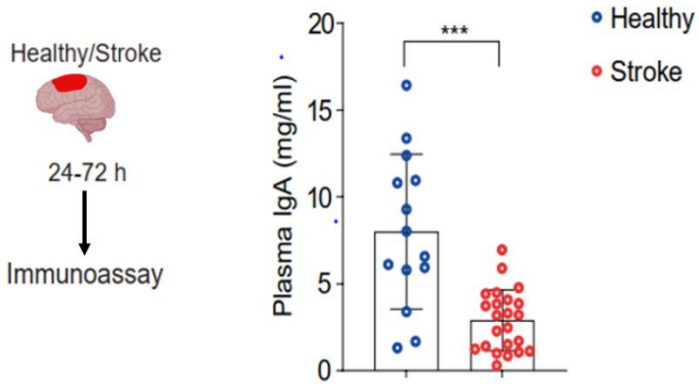

Figure 6: Stroke induces reduction in plasma IgA levels. A Concentrations of plasma IgA in stroke patients and healthy controls measured by ELISA (n=14-23 per group).

To investigate the effect of ischemic stroke,circulating IgA levels were measured with an immunoassay. Stroke patients' blood was collected within the first 72 h of symptom onset, which was followed by plasma isolation. Afterwards, the levels of plasma IgA in stroke patients and age-sex matched healthy controls were quantified to understand whether ischemic stroke regulates IgA levels. Indeed, within 72 h of stroke onset, ischemic stroke patients showed lower plasma IgA levels compared to healthy controls, indicating a dysbalance in mucosal immunity (Fig. 2).

4.2. Ischemic stroke promotes the release of neutrophil extracellular traps

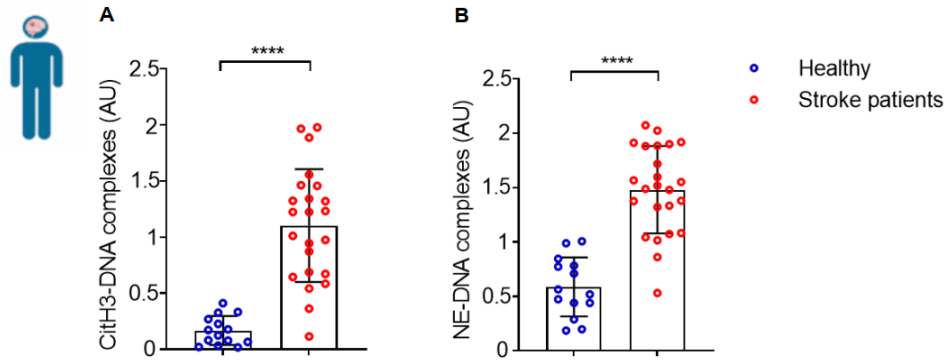

Figure 7: Stroke patients show higher levels of NETs in plasma. A, Relative plasma levels of citH3-DNA and B, NE-DNA complexes in stroke patients and healthy controls (n=14-25 per group).

Several preclinical studies have shown the fundamental role of neutrophils in stroke pathophysiology (Kang et al., 2020, Neumann et al., 2015). Furthermore, when neutrophils are activated, they release NETs, which could potentially lead to the blockade of microvessels in the brain (Kang et al., 2020). In addition, activated neutrophils might have detrimental effects in the circulation, as soluble mediators are found in the blood stream, further activating neutrophils. These soluble mediators might be related do dying neurons after ischemia or activated platelets as a result of hypoxia in the vasculature (ChenKang and Tang, 2022). Hence, plasma NETs markers were measured in stroke patients, within 1-3 days of stroke onset. NETs are composed of DNA strands decorated with cit-H3, NE, myeloperaoxidase (MPO) and Histone H4, to name the central components (Tsourouktsoglou et al., 2020, Urban et al., 2009). Measuring the activity or release of NETs is thus possible via ELISA, combining the characteristics of DNA strands with cit-H3 or NE for identification as NET component. Therefore, an ELISA was designed with a plate coated with an antibody against cit-H3 and a second ELISA with anti-NE as antibody. As NETs need to have both the histones or enzymes with DNA strands, a detection antibody against DNA, that is labeled with enzyme (horse radish peroxidase - HRP)was used, further incubated with substrate to measure the activity of the enzyme, the signal of which is then directly correlated to the NET amounts present in the sample. Compared to healthy controls, stroke patients had significantly higher levels of Cit-H3-DNA and NE-DNA complexes, indicating more release of NETs into the blood

stream by activated neutrophils (Fig. 3A, 3B).This indicates a potential role of NETs as soluble mediator. Next to direct brain damage induced by NETs, the focus of previous studies, additional effects could be observable outside the brain.

4.3. Increased amounts of NETs negatively correlate with plasma IgA levels in stroke patients

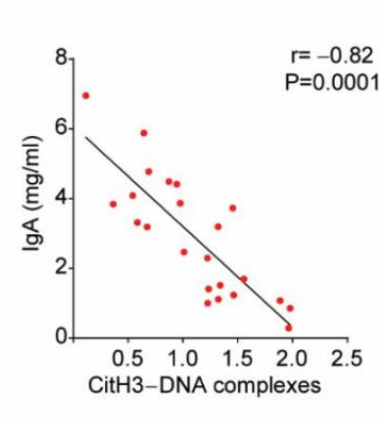

Figure 8: Correlation between plasma citH3-DNA complex levels and IgA amounts in stroke patients (n=23).

The activation of neutrophils and the release of neutrophil extracellular traps (NETs) occur within the same timeframe as the observed decrease in IgA levels in the plasma of these patients. This led to an investigation into a possible correlation to uncover any further interactions. Interestingly, it was found that higher levels of NETs in the plasma were associated with lower levels of IgA (Fig. 4). This observation is the first time that the appearance of NETs is associated with the suppression of key elements of the peripheral immune system, which is commonly observed in stroke patients. Yet, this correlation needs to be proven with a causal relation between NETs and circulating IgA.

4.4. Experimental stroke in mice induces shrinkage of Peyer's patches

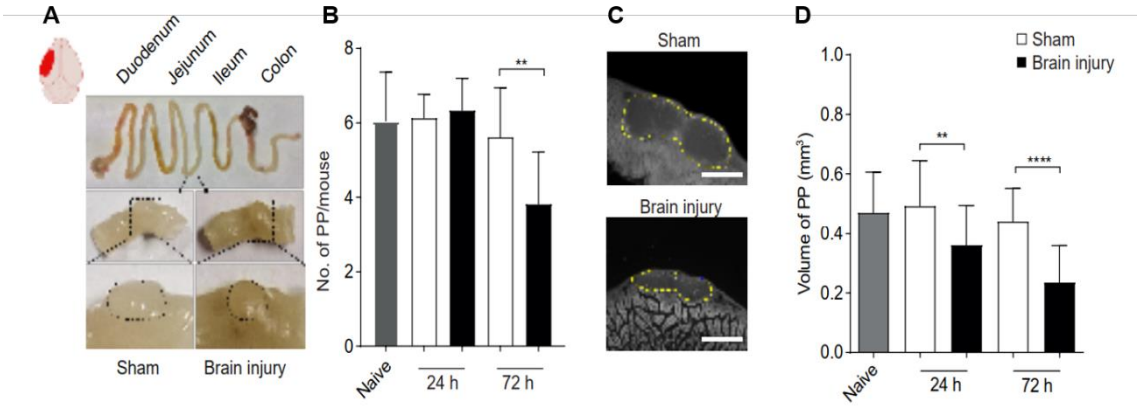

Figure 9: Experimental stroke induces size reduction in PP. A, Macroscopic overview of the mouse gastrointestinal tract with the demarcation of PP one day after sham surgery or stroke. B, Number of PP in small intestine in naïve, 24 h and 72 h post-stroke and sham surgery mice. C, Representative LSFM autofluorescence images of cleared intestinal PP showing their shrinkage 24 h after stroke compared to sham control, scale bar=500 µm. D, Volume analysis of whole PP 24 h and 72 h after sham or stroke; (n=23 PP for sham and n=16 PP for stroke, n=3-4 mice for 24 h and n=34 PP for sham and n=24 PP for stroke, n=6 mice for 72 h).

Peyer's patches are major sites for the priming of intestinal immune cells, especially B cells, with microbiota leading to B cell development into plasma cell precursors (Reboldi and Cyster, 2016). As plasma cells secrete IgA and IgA levels were lower in patients with stroke, a mouse model of stroke was used to assess the effect of ischemic stroke on Peyer's patches. After stroke, Peyer's patches were isolated from small intestine, and during the process of dissection, smaller PPs were observed in the stroke-induced mice (Fig. 5A). Furthermore, the number of harvested PPs were quantified after 1 or 3 days after stroke, showing a decrease after 3 days, which was caused by the shrinkage of PPs, that made it imposible to harvest or analyze the then almost invisible PPs (Fig. 5B). A detailed analysis via whole organ imaging was chosen to procede, as PPs are complex structures with varying sizes and morphologies. Yet, in the literature, a previous protocol was not described for light sheet fluorescence microscopy imaging of PPs. As a first step, unstained PPs were imaged and autofluorescence (AF) of those gastrointestinal tract fragments was used for the analysis of whole PP volumes. Paralleling our observations during dissection, the volume of PPs were decreased after 1 and 3 days of stroke induction (Fig. 5C,D).

4.5. Stroke induces B cell follicle shrinkage in Peyer's patches

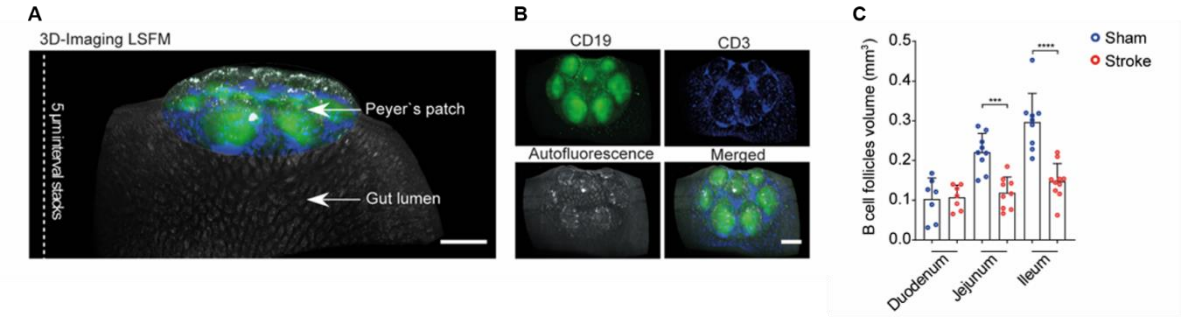

Figure 10: Stroke induces B cell follicle volume shrinkage in PP. A, Fluorescence images after 3D reconstruction of stained PP showing the position of PP in the small intestine that were whole-mount stained with anti-CD19 (green) and anti-CD3 (blue) fluorescent antibodies before clearing and LSFM, scale bar= 500 µm. B, Fluorescence single-channel and merged images are shown, scale bar=500 µm. C, Machine learning-based automated analysis of B cell follicle volume in PP from duodenum, jejunum and ileum one day after stroke or sham (n=7-11 PP per intestinal segment, 4-6 mice per group).

Even though total volume of PPs were decreased, a thorough analysis of cell subsets in the PPs was necessary to understand, whether the volume decrease was a result of B cell loss, causing a potential decrease in IgA levels. 3D LSFM imaging of PPs was established via modification and optimization of previous protocols, as this study is the first to perform a whole organ imaging of PP, enabling the possibility to observe and quantify B and T cell subsets in PPs (Renier et al., 2014). The imaging pipeline was established with CD19, CD3 and AF imaging, AF defining the gut morphology (crypts etc.), whereas $CD19^+$ signals showed a B cell follicle structure, which was surrounded by $CD3^+$ T cell zones (Fig. 6A). To further elucidate and analyze the LSFM images, a machine-learning based algorithm and human-in the loop system were introduced.

B cell follicle volumes in duodenum were not altered after stroke, whereas the PP B cell follicles in jejunum and ileum were significantly smaller. As B cells contribute around 70-80% of the PP cell composition, the shrinkage of the PP was attributed mainly to B cell loss (Fig. 6B). As PP B cells are main precursors of IgA producing plasma cells, B cell loss in PP may be the pathophysioloical explanation of IgA loss after stroke.

4.6. Stroke differentially impacts lymphocytes numbers in lymphoid tissues

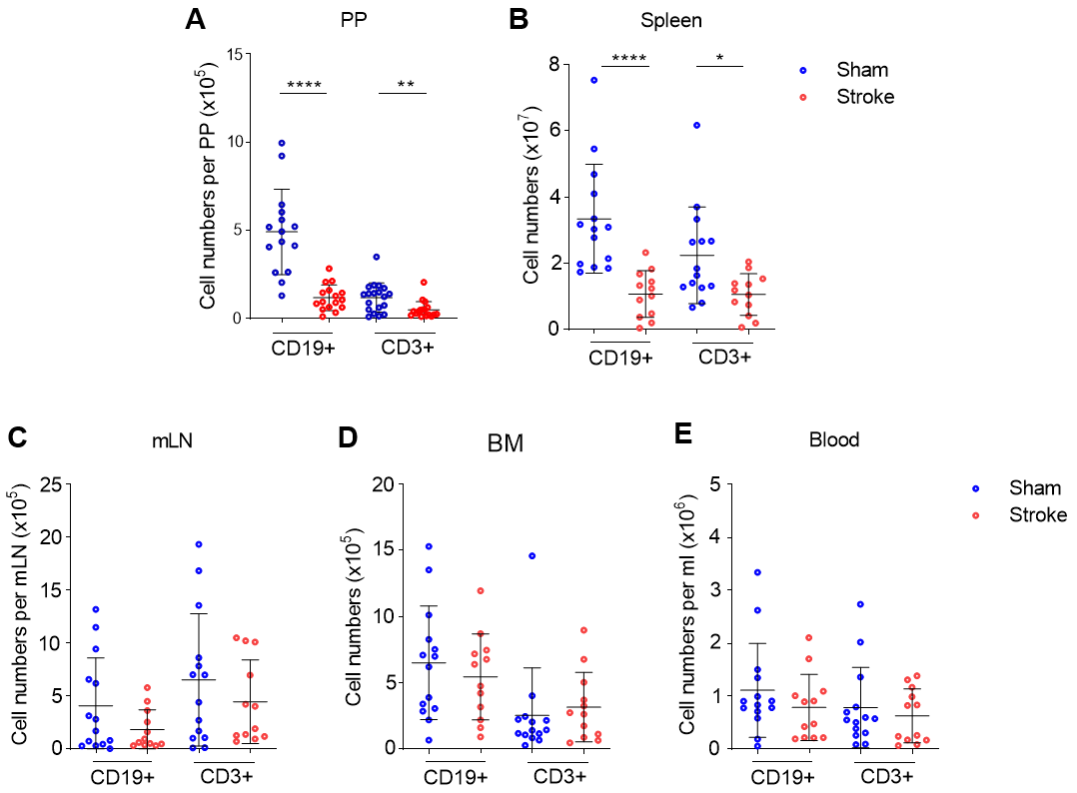

Figure 11: Total numbers of CD19$^+$ B cells and CD3$^+$ T cells 24 h after stroke or sham surgery, in PP (A), spleen (B), mesenteric lymph nodes (mLN)(C), bone marrow (BM)(D) and blood (E) (n=12-13 mice per group).

To further elucidate lymphocyte regulation after stroke, multiple systemic immune organs were analyzed via flow cytometry. Similar to the LSFM data, flow cytometry also showed a strong decrease in B cell numbers after stroke in PP (Fig. 7A). Furthermore, the B and T cell numbers in spleen were decreased, as also shown in previously published data (Fig. 7B) (Roth et al., 2021). Nevertheless, in other organs such as mesenteric lymph nodes or bone marrow, there was no significant difference in CD19$^+$ B cell numbers after stroke (Fig. 7C,D,E). These results suggest a differential impact of stroke on lymphocytes in systemic immune organs, especially in spleen and in PP.

4.7. Stroke induces PP shrinkage in hypercholesterolemic mice

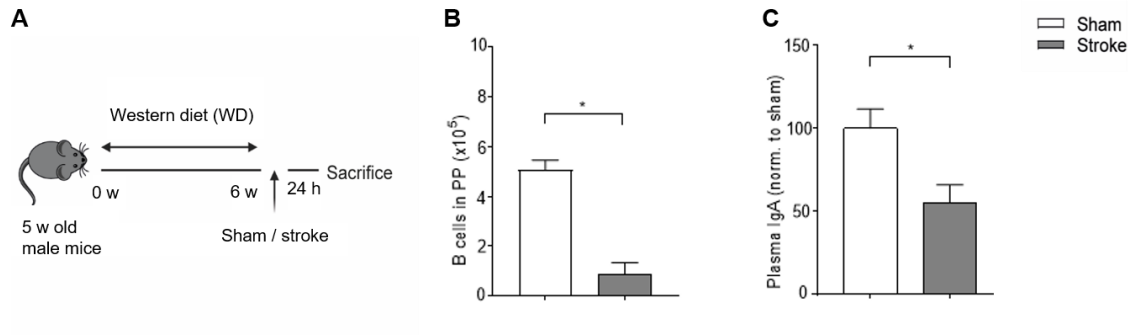

Figure 12: Stroke induces B cell loss and less plasma IgA concentrations in hypercholesterolemic mice. A, Experimental paradigm showing the treatment of mice with WD and the induction of stroke or sham surgery. The numbers of B cells in Peyer's patches (B) and plasma concentration of IgA (C) in WD mice 24 h after sham or stroke surgery (n=4 mice per group).

Patients with comorbidities are more prone to stroke occurrence and have worse prognosis. Among those comorbidities, hyperlipidemia is a strong predictor for cardiovascular disease and it causes endothelial damage and vasomotor activity dysfunction- in which both are pathophysiological mechanisms of hypertension, which is another risk factor of stroke occurrence and a predictor of bad prognosis after stroke (Nelson, 2013). Hence, hyperlipidemia is a major contributing factor to stroke related mortality and morbidity worldwide (She et al., 2022). As a risk factor, hyperlipidemia can be mimicked in animal models to understand the underlying pathophysiology, leading to higher stoke incidence and bad prognosis. These preclinical studies have shown worse prognosis after 1 and 3 days after stroke, which was shown to be related to higher neutrophil infiltration into the stroke affected areas. Even though most of the preclinical stroke studies utilize tMCAO in healthy young mice, it is crucial to validate the findings in mouse with comorbidities. Hence, Western diet was provided to wild type mouse to induce hyperlipidemia. 24 h of reperfusion was followed by sacrifice and Peyer's patch isolation to validate the results in normolipidemic wild-type mice described above (Fig. 8A). $CD19^+$ B cell numbers were quantified using flow cytometry. After 24 h of reperfusion, hyperlipidemic stroke mice showed decreased number of B cells in PP, in comparison to sham mice with hyperlipidemia (Fig. 8B). This result is in parallel with the normolipidemic mouse LSFM and flow cytometry data. Furthermore, plasma IgA concentrations were measured in WD mice. 24 h after stroke, WD mice showed less

plasma IgA in comparison to WD sham mice, indicating a potential relation between PP B cell decrease, plasma IgA loss and neutrophil activation as described above (Fig. 8C).

4.8. Western diet induces hypercholesterolemia

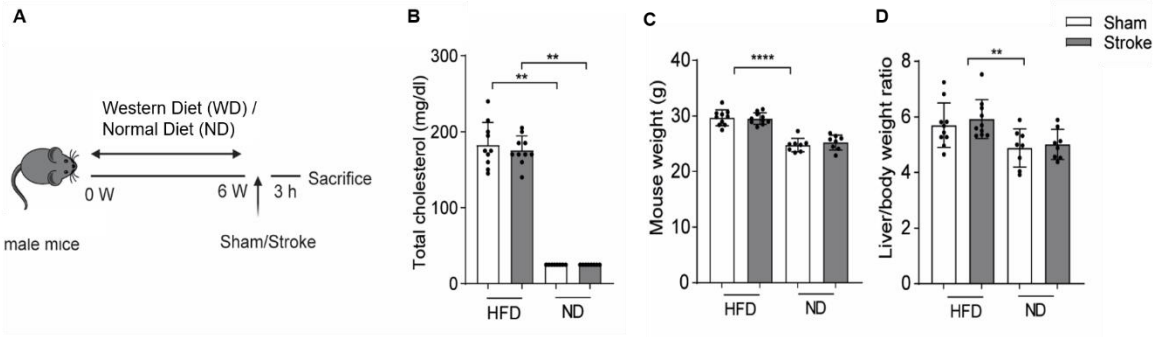

Figure 13: Western diet induces metabolic alterations in wildtype male mice. A, Experimental paradigm showing the treatment of mice with WD or ND and the induction of stroke or sham surgery. The plasma concentrations of cholesterol (B), body weight (C) and liver/body weight ratio (D) in WD and ND mice 3 h after sham or stroke surgery (n=8-10 mice per group).

Mice with hyperlipidemia were subjected to stroke surgery and showed reduced numbers of B cells in PP after 24 h of reperfusion, which might be caused by neutrophils as correlated in human subject samples. Even though immune cell regulation is observed within 24 h, neutrophils have shown to be one of the early activated immune cells after stroke (Gelderblom et al., 2009). In this regard, the study focused on neutrophil activation at an earlier time point. As current stroke treatment guidelines recommend treatment to be given within 4,5 hours of stroke onset (therapeutic window), it is crucial to understand the regulation of immune system, especially neutrophils, within this time period to target certain characteristics of neutrophils in patients with hyperlipidemia specifically within therapeutic window. However, the early activation pattern of neutrophils in hyperlipidemic individuals was not investigated, neither in clinical nor preclinical models, unraveling whether patients with comorbidities have more detrimental effects coming from neutrophil hyperactivation, which might result in potential side effects.

To mimic clinical conditions, Western-style high sugar and fat diet (WD) was provided to mice ad libitum for 6 weeks (Fig. 9A). For the control group, normal chow was

provided, and both groups were followed for general health conditions during treatment. As previously described, WD induced higher body weight and liver/body weight ratio compared to ND mice. In addition, WD mice showed elevated total cholesterol levels, mimicking the clinical risk factors *in vivo* (Fig. 7B-D).

4.9. Stroke induces early neutrophil activation

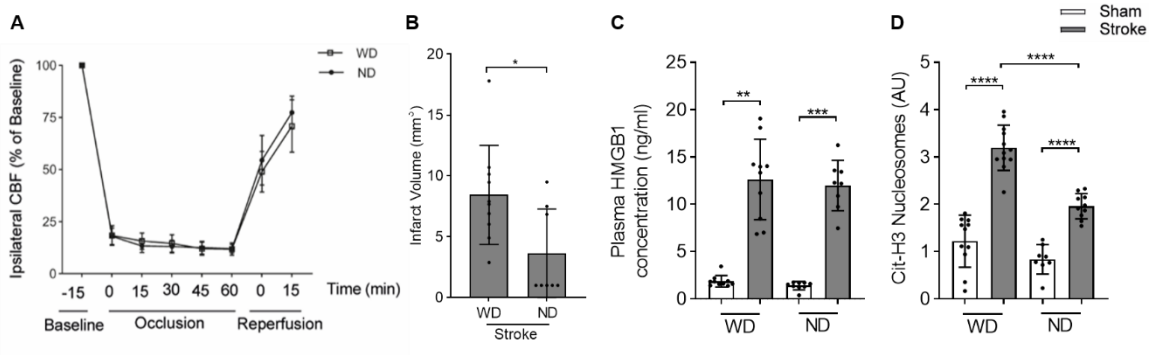

Figure 14: A, Cerebral blood flow (CBF) measurements by doppler recordings during ischemia-reperfusion injury in WD and ND mice. B, Quantification of brain infarct volumes using cresyl violet stained histological brain sections in WD and ND mice. Plasma HMGB1 concentrations (C) and citH3-DNA nucleosome relative comparisons (D) were measured via ELISA in WD and ND 3 h after stroke and sham surgeries (n=8-13 mice per group).

Following WD, previously described mouse model of ischemic stroke was utilized (see sections 4.5 and 5.4). After surgery, a timepoint of 3 h (which is within therapeutic window) was selected to investigate the activation pattern of neutrophils and brain injury. Hence, 3 hours after stroke, the mice were sacrificed and organs were harvested. Occlusion of MCA resulted in a reproducible decrease in cerebral blood flow, did not significantly differ between WD and ND mice (Fig. 10A). However, mice fed on WD showed significantly increased infarcts compared to ND mice (Fig. 10B).

Innate immune cells, especially neutrophils, mediate early cellular immune activity. This starts with the activation of neutrophils, which was shown to be induced by high mobility group box 1 (HMGB1) (Denorme et al., 2022). Platelets are activated after stroke by the release of von Willebrand factor (vWF) from damaged endothelium, by released reactive oxygen species (ROS), or by the collagen (Pawlinski, 2016, Yun et al., 2016). Activated platelets then release HMGB1in response to those stimuli.

To quantify the inducer of neutrophil activation, an HMBG1 ELISA protocol was established. This immune assay enables the quantification of the released HMGB1 after stroke, both in WD and ND groups. In both feeding groups, stroke mice showed increased circulating levels of HMGB1, showing activated platelets and the potential to induce neutrophil activation. Yet, HMGB1 levels were not significantly different between WD and ND stroke mice (Fig. 10C).

As activated neutrophils release NETs, we wanted to see whether increased HMGB1 concentrations were accompanied by a release of NETs. Hence, we investigated the characteristics of circulating DNA in WD and ND stroke mice, which included the presence of citH3 bound to DNA strands. Quantification of citH3-nucleosomes revealed increased levels of NETs in stroke mice compared to sham. Interestingly, this increase was even more upregulated in the WD stroke group in comparison to the ND stroke mice (Fig. 10D).

4.10. Western Diet modulates neutrophil dynamics in stroke mice

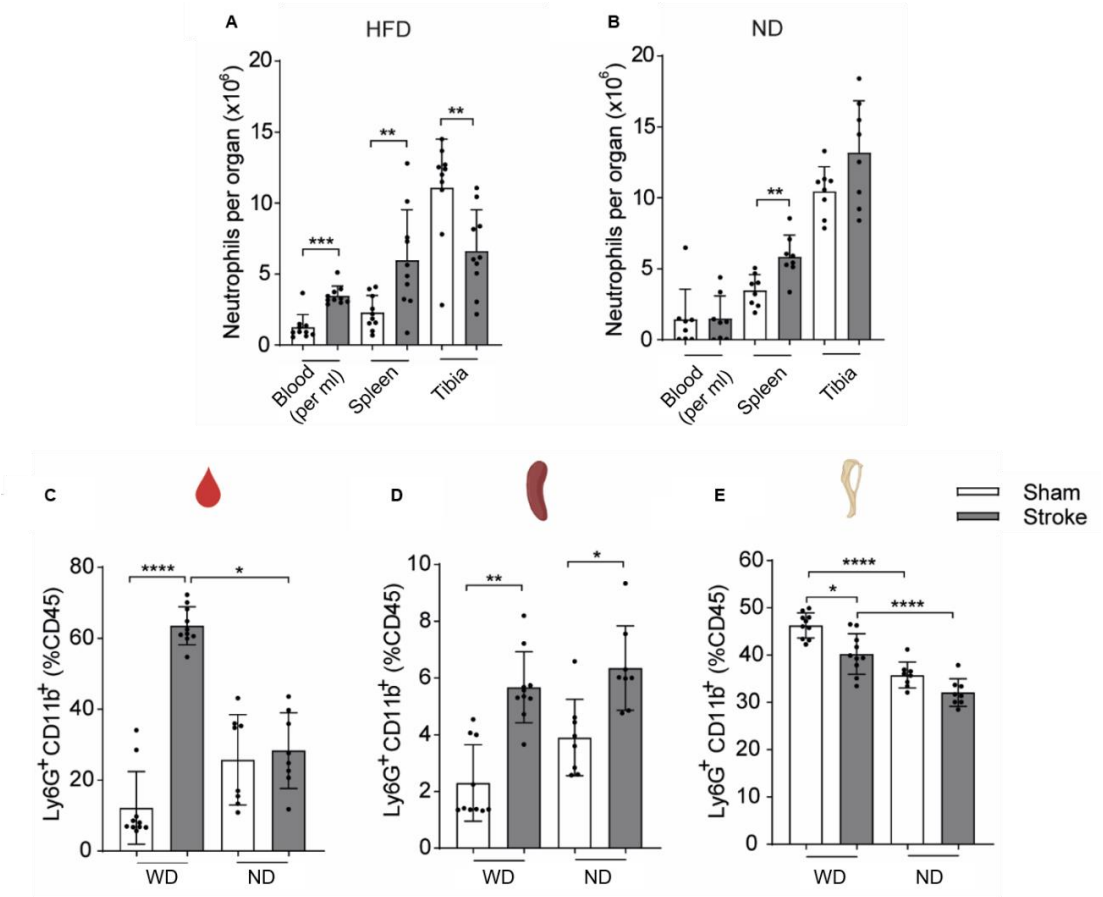

Figure 15: Neutrophil numbers per ml blood, per spleen and per tibial bone marrow in WD (A) and ND (B) mice 3 h after stroke and sham surgeries. Frequency of neutrophils in blood (C), spleen (D) and tibial bone marrow (E) in WD and ND mice 3 h after stroke and sham surgeries (n=8-10 mice per group).

Next, as the innate immune cells were found to be related with an adverse outcome of stroke in WD diet mice in previous studies and neutrophil activation was observed in the current study; the total numbers of neutrophils in systemic immune organs, including blood, spleen and bone marrow were quantified to understand the dynamics of cell mobilization after stroke. Interestingly, WD stroke mice showed significant increases in neutrophil numbers as well as percentages in blood and spleen compared to the WD sham group (Fig. 11A, C, D); whereas this effect was only observed in the spleen of ND mice (Fig. 11B, D). In contrast, bone marrow neutrophils were decreased in WD stroke mice, which might be related to a potential mechanism of early release of neutrophils from the BM to the circulation or marginalization from other organs (Fig. 11A). Of note, the

percentage of neutrophils in the BM of WD group mice was significantly higher than in ND animals-proposing a higher neutrophil frequency in WD mice (Fig 11E). After activation and egress from BM, these data suggest an early activation of neutrophils in the acute phase of stroke, which is worsened by WD.

4.11. Western Diet but not stroke increases expression of neutrophil activation receptors

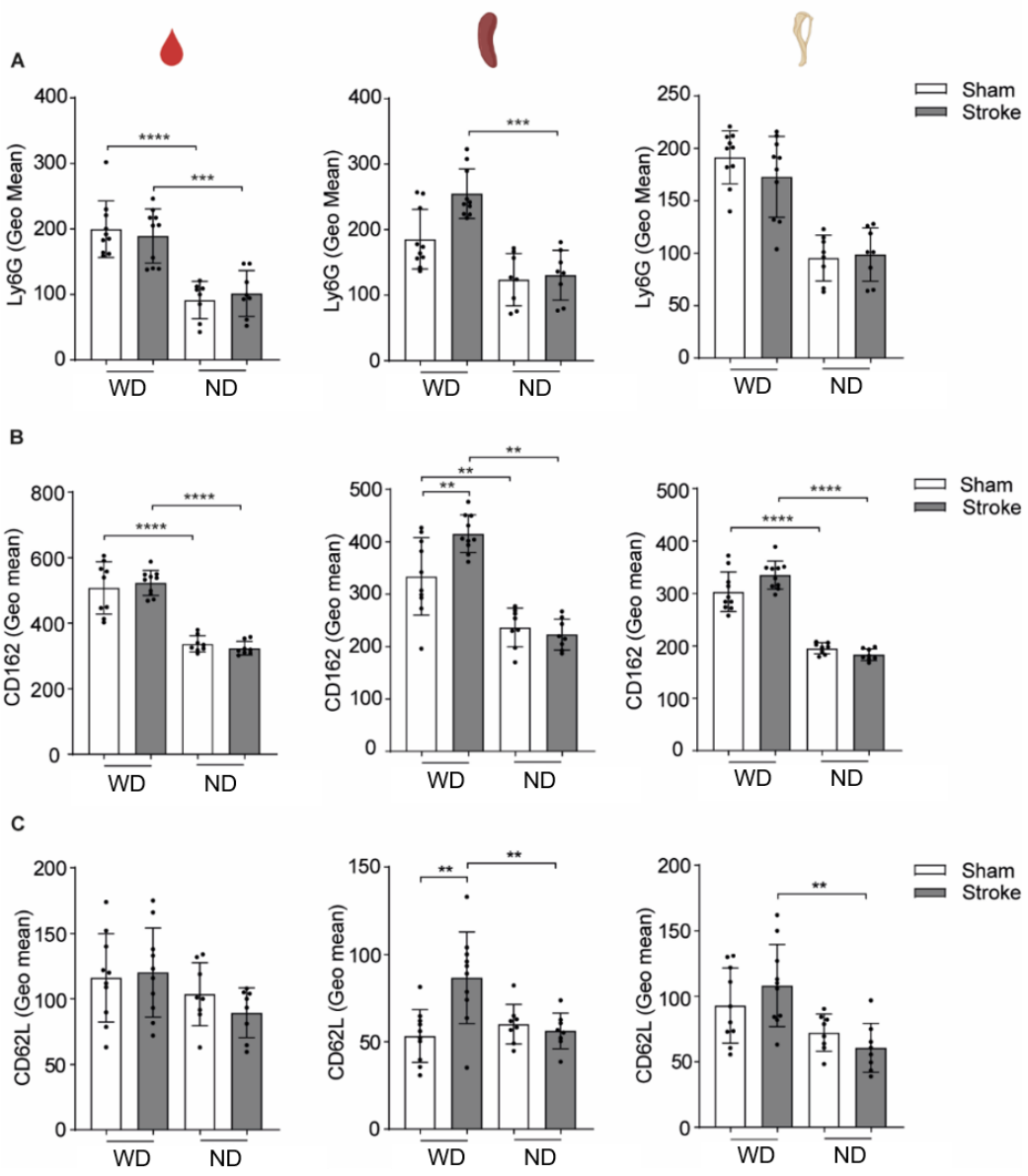

Figure 16: Mean receptor expression of Ly6G (A), CD162 (B) and CD62L (C) in blood, spleen and tibial bone marrow neutrophils of WD and ND mice 3 h after stroke or sham surgery (n=8-10 mice per group).

To determine the activation pattern of innate immune cells in systemic immune organs in detail, a thorough investigation of activation, migration and adhesion receptors via flow cytometry was employed. First, neutrophils were analyzed as first invaders of the ischemic brain and cells that release NETs. In WD mice, neutrophil migration and activation were upregulated in blood and spleen, whereas there was no difference in Ly6G expression between sham and stroke groups, indicating an effect of diet on neutrophil regulation (Fig. 12A). Furthermore, in spleen, neutrophil maturation was higher in WD mice after stroke compared to sham or ND (Fig. 12A). In contrast, no difference was seen in the blood and only the WD stroke group showed higher maturation levels in comparison to the ND stroke group (Fig. 12A). Next, we studied the changes in the adhesion receptor CD162, which drives and initiates neutrophil tethering and rolling along lumen of vessels (Rolfes et al., 2021). CD162 was upregulated in the WD group in comparison to ND in all organs, indicating more and blocking cascade in the vasculature in several organs (Fig. 12B) (Jickling et al., 2015). Previous studies have shown higher percentage of blood neutrophils expressing CD62L in response to stroke with a lesser mean expression of the same receptor, showing more activation (Rolfes et al., 2021). Yet these studies were mostly conducted 24h after stroke. In our study, there was no difference in the expression of CD62L in blood, whereas it was upregulated in WD stroke group in BM and spleen, showing less activation (Fig. 12C). Further studies are needed to understand the mechanism behind this differential regulation.

4.12. Hypercholesterolemia induces early proinflammatory cytokine release after stroke

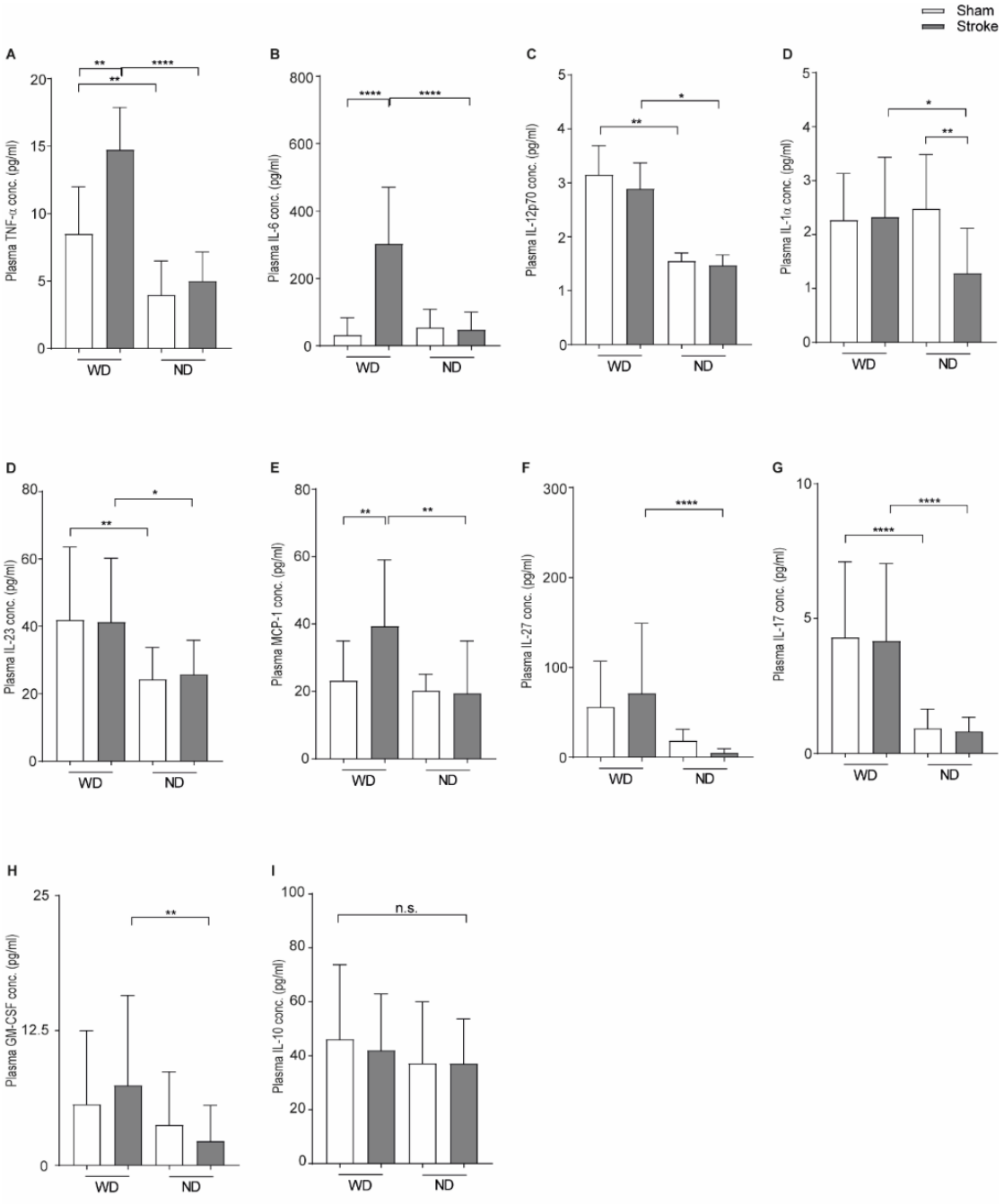

Figure 17: Plasma concentrations of TNF-a (A), Il-6 (B), Il-12p70 (C), Il-1a (D), Il-23 (D), MCP-1 (E), Il-27 (F), Il-17 (G), GM-CSF (H), Il-10 (I) 3 h after stroke or sham surgery in WD or ND mice (n=8-10 mice per group).

Stroke promotes cytokine release, causing innate immune cell activation. These activated immune cells start releasing a plethora of cytokines that in return cause a general immune activation and inflammation. Hence, it is crucial to investigate the cytokine levels in different groups that are investigated during the current study. Activated neutrophils might secrete cytokines, in addition, other immune cells might release cytokines that induce more neutrophil activation. Similar to immune activation regulation with different diets, cytokine levels in plasma and different tissues might be differentially regulated after stroke and different diet regimes.

To further investigate the hyperacute cytokine regulation after stroke, we implemented a previously described method to analyze 13 different inflammatory cytokines (Sposito et al., 2021). These proinflammatory cytokines play a role in innate immune activation, T cell induction or immune cell egress from the bone marrow; which is balanced by anti-inflammatory cytokine release under physiological conditions.

TNF-α is one of the most intensively investigated cytokines after stroke, often released by monocytes, indicating inflammation and tissue damage (Jang et al., 2021). 3 h after stroke, WD stroke mice had significantly higher TNF-α levels than WD sham and ND stroke mice (Fig. 13A). Another cytokine, that was shown to recruit neutrophils and induce inflammation was IL-6, which was upregulated in WD stroke mice, indicating a potential worse prognosis at later timepoints (Fig. 13B) (Zhu et al., 2022). Furthermore, one of the innate immune response regulators, IL-12p70 (commonly designated IL-12), was upregulated in WD groups, indicating a general proinflammatory effect of WD (Fig. 13C). On the other hand, these effects were absent in IL-1α levels (Fig. 13D) (Zhu et al., 2022).

Proinflammatory cytokines play a crucial role in the activation of adaptive immune responses via T cells. IL-23, inducing the development of proinflammatory Th17 cells, was upregulated in WD groups; but there was no difference between sham and stroke mice (Fig. 13D) (Gaffen et al., 2014). Yet, MCP-1 and IL-27 were both increased in WD stroke mice, having a role in monocyte recruitment and T cell induction (Fig. 13E, F). In return, activated T cells also release cytokines, such as IL-17, which was shown to recruit more innate immune cells and be detrimental in stroke outcome (Singh et al., 2016). IL-17 was upregulated in WD groups in comparison to ND (Fig. 13G).

GM-CSF stimulates monocytes and macrophages to secrete proinflammatory cytokines, it also induces immune cell egress from bone marrow (LeeAchuthan and Hamilton, 2020). After stroke, WD mice showed higher levels of GM-CSF, which might be the reason of higher neutrophil numbers observed in blood and spleen (Fig. 13H). Furthermore, sustained GM-CSF levels might cause more neutrophil release in the course of post-stroke inflammation, increasing neuroinflammation and damage. Further studies are needed to understand the time-course of the concentrations of GM-CSF and other cytokines to understand long term effects of WD and stroke. In addition to increased levels of proinflammatory cytokines, there was no anti-inflammatory IL-10 peak in stroke mice, indicating disbalance of cytokines to a shift towards proinflammation (Fig. 13I).

5. Discussion

Stroke is the second most common reason of mortality and morbidity in the world. In 2019 more than 120 million-person years were lost by the disability in patients with stroke (Collaborators, 2021). Yet, within the last decades no new targeted therapy against ischemic stroke or related complications has been approved. The total number of affected people is expected to increase in the upcoming years, as a result of longer life expectancy and higher population, despite better and quicker access to health care services (Collaborators, 2021). These conditions altogether show the need for new efficient treatment paradigms. Unraveling the pathophysiology of not only ischemic stroke itself, but also the post-stroke complications and comorbidities is the most logical way to deliver better algorithms of short- and long-term stroke treatment.

Stroke treatment not only includes reperfusion (thrombolysis or thrombectomy), but also the management of complications following the stroke event. Of those, more than 30% are related to the immune system or infections (Bathla et al., 2023). Being activated after stroke, immune cells migrate into the brain and cause inflammation, which may damage the local cells. However, these inflammatory and resolving processes are also required for better recovery after stroke. On the other hand, activated immune cells are first found in the blood and then migrate into the brain. During this process, several DAMPs are released, causing side effects of immune regulation, namely immunosuppression. The initiation and effect of immunosuppression might be related to worse clinical outcome after stroke. One of the most common complications is pneumonia. Furthermore, other mucosal barriers, e.g. in the urinary or gastrointestinal tract might suffer from infection or bleeding following stroke (Collaborators, 2021). All those organs have mucosal surface damage in common. Hence, the aim of this study was to first understand, whether the amounts of IgA are changed after stroke, as IgA is the most abundant immunoglobulin in mucosal surfaces. Therefore, blood samples from stroke patients and age-sex matched controls were collected. Afterwards, ELISA measurements were done to evaluate the regulation of IgA. Within first week of stroke, IgA levels in plasma were reduced in stroke patients, compared to healthy controls. Yet, this study did not measure the mucosal surface bound IgA regulation in the lungs directly, as bronchoalveolar lavage (BAL) after

stroke is a risky and stress-inducing procedure, that might worsen clinical outcome in patients. Further clinical trials/studies investigating organ specific regulation of IgA might increase the understanding of IgA regulation after stroke. Yet, plasma IgA level measurement is a cost-effective and rapid way to foresee the IgA regulation after stroke, also indicating changes in the mucosal surfaces. While taking blood samples for daily routine controls of patients in the inpatient clinic, small volumes can be reserved and isolated plasma can be used, not only for the measurements of IgA levels but also of immune cell activation markers such as citH3-DNA and NE-DNA in the plasma, which in this study stood for neutrophil activation. Moreover, experimental preclinical models of stroke might be used to investigate organ-specific changes to understand IgA regulations after brain ischemia. Thereby, BAL collection, histological analysis and infection models can be used to investigate the spatial regulation of IgA in a time-course manner. However, these experimental paradigms are beyond the aim of current study.

Previous studies have shown the role of neutrophils after stroke, infiltrating the brain as first peripheral immune cells and accelerating inflammation, later on inducing other immune cells to infiltrate and further resolution of inflammation (Cai et al., 2020). Yet, this study revealed the early activation of blood neutrophils, releasing NETs in response to sterile injury. It is plausible to state that this activation pattern is further continued during stroke progression, with different subsets of neutrophils at different activation states, such as migrating into brain, extravasating or releasing NETs at different sites. However, it is not previously described, whether these neutrophils might cause damage and promote inflammation in the blood stream or peripheral organs. On the other hand, it has previously been described that cell free DNA (cfDNA) in the blood might induce macrophage activation and splenic T cell death after stroke, causing immunosuppression and increased infections- though the source of cfDNA in this study was not investigated (Roth et al., 2021). Interestingly, cfDNA peak showed by Roth et al. was at 6 hours post stroke in plasma, which coincides with the activation time of neutrophils found in the current study. As NETs also include DNA strands, it is plausible to state a direct relation between the neutrophil activation, NETs release and cfDNA increase in blood, yet further experiments are needed to understand, whether this observation possesses a causation.

Interestingly, the time frame of neutrophil activation and NET release paralleled the IgA drop in the plasma of the stroke patients. To further analyze, correlation and regression tests were performed and a negative linear correlation was observed between NETs and IgA levels. Moreover, a significant linear correlation was followed by a Spearman regression. In this analysis, the citH3-DNA and IgA quantities were used from the same patient in the same time point. However, this correlation cannot reveal a causation between NETs and IgA level changes after stroke. Therefore, further studies are needed to understand, whether NETs directly cause IgA masking or decrease their production. Furthermore, NETs might diffuse into some tissues and cause cell death in IgA production sites. It has been shown before that histone H4, which is part of NETs, can induce chronic inflammation and induce cell death (Silvestre-Roig et al., 2019). DNA fragments in combination with citrullinated-Histone 3 were also shown to be pro-inflammatory (Tsourouktsoglou et al., 2020). After stroke, it is known that gut barriers are damaged and tight junctions are also "leaky" (Sugiyama et al., 2023). Stroke might cause vascular permeability increase as a result of increase in sympathetic system, or via inflammation. Overall, these conditions might make PP susceptible for NET entry, which can induce cell loss in PP. Moreover, NETs are recognized via TLR2 or TLR4, which are found on lymphocytes, with the possibility to "sense" the NETs release and be activated to kill or phagocytose other cellular compartments, as similarly shown by macrophages sensing cfDNA in spleen and inducing T cell death (Roth et al., 2021, Tsourouktsoglou et al., 2020, Silk et al., 2017). Neutrophils migrating to non-specific tissues and releasing NETs in those organs is another plausible hypothesis that needs to be experimentally tested.

To further elucidate the potential role of neutrophils in IgA drop, we implemented a well-established mouse model of stroke, namely transient middle cerebral artery occlusion. This method enables to mimic the induction of tissue ischemia for a controlled duration (e.g. 30-45-60 minutes), which is followed by the filament removal, mimicking reperfusion in the clinics. In parallel to our clinical data, we saw reduced IgA levels in mice within 24h of stroke. In order to understand the regulation of IgA production, 3D imaging via LSFM was implemented. After protocol optimization, total Peyer's patch volumes were measured. The observation of reduced PP volumes was supported by whole mount staining to have cell type specific quantifications. B cell volumes in PPs, especially

in jejunum and ileum were decreased after stroke, indicating a site- and cell type-specific regulation of PP morphology. As PP B cells are precursors of plasma cells, which produce IgA, this observation of early PP shrinkage might be the reason of reduced IgA levels. Yet, this observation needs to be supported via flow cytometry, histology or other techniques to dissect the regulation in a time span and mechanistic manner. Further experiments elucidating the early activation of neutrophils in the mouse model of stroke, later on inhibition of NETs release and protection of intestinal physiology and antibody production need to be investigated in further experimental settings. This activation pattern of neutrophils and decrease in B cell numbers strengthens the possibility of NETs to be migrating into peripheral tissue or inducing cell death via circulation- without masking already secreted IgA.

Hypercholesterolemia and obesity are major risk factors for stroke, leading to higher morbidity and mortality. However, current guidelines only include standard treatment modalities, namely thrombolysis and thrombectomy, without any additional acute intervention for patients with comorbidities (Berge et al., 2021, Turc et al., 2023). Modification of lifestyle or dose management of antihyperlipidemic medications only show long-term effects, eliminating the possibility of being beneficial against acute inflammatory damage. Hence, the characterization of early responses within the therapeutic window in stroke patients with comorbidities is needed to define key regulators of stroke outcome. In addition, preclinical studies usually include healthy young mice due to handling and post-stroke care comforts. Studies with hyperlipidemic mice often prefer only knockout models (e.g. ApoE), which may not reflect the human prevalence of risk factors, as monogenic obesity only accounts for 5% of the population. Thus, in the current study, mice were provided with a high-fat and sugar diet, namely Western diet to investigate the role of WD on stroke with wild-type mice. In the same direction as normolipidemic WT mice, WD fed mice also showed less numbers of B cells in the PP, with a potential relation to decreased levels of plasma IgA. To further investigate the immune regulation in WD mice, we focused on neutrophils, which are one of the first immune cells to react upon stroke induction. Hence, an earlier time point was selected to investigate neutrophil activation patterns in WD and ND mice after stroke.

Treatment of stroke is established with the motto “time is brain”, as earlier interventions with thrombolysis and thrombectomy have better outcomes. These approaches are applied within a therapeutic window of 4.5 hours after first symptom onset (Berge et al., 2021). Thus, our experimental paradigm in the second set of experiments investigated the effect of hypercholesterolemia within this window, focusing on 3 hours after stroke initiation.

The current study reveals the effect of stroke and WD on innate immune cells at the hyperacute phase. Three hours after stroke, neutrophils are more proinflammatory, activated and adhesive in WD animals, showing a hyperactivation pattern. Conversely, at this time point, neutrophils of ND animals do not show the same overactivation pattern in comparison to sham surgery. One of the main inducers of this activation pattern is the platelet-released HMGB1, resulting in induction of NETs release from neutrophils after stroke. There is an increase in HMGB1 levels after stroke, without a difference between WD and ND groups. Yet, NETs were released more from the neutrophils of mice fed with WD. Platelet derived HMGB1 was shown to be the regulator of NETs release after stroke (Denorme et al., 2022). As HMGB1 levels in plasma were not significantly different in WD and ND stroke groups, it is plausible to state an overactivated response of neutrophils in response to the same stimulus with certain characteristics. As previously reported, hyperlipidemia induces neutrophil activation in steady state, with endothelial invasion and damage, which is in parallel to the current results, showing more activation in hyperlipidemic mice in comparison to ND mice (Drechsler et al., 2010). Furthermore, in blood, stroke mice show a further increase in receptors related to maturation and T cell induction, indicating a general overshooting of the innate immune system at the hyperacute phase of stroke.

The activation patterns of innate and adaptive immune cells depend on cytokines, which are released after stroke. WD stroke mice had more proinflammatory cytokines, that were not only released by monocytes and T cells, but also in return inducing innate and adaptive immune cell activation. More GM-CSF was detected in WD stroke mice, that might be causing increased neutrophil numbers after 3 h of stroke and constant egress to blood. While proinflammatory cytokines were increased significantly, anti-inflammatory

cytokine levels were not differentially regulated. Interestingly, ND mice did not show an increase in cytokine levels as WD mice did. This cytokine regulation pattern was in the same direction as receptor regulation of innate immune cells, showing less hyperactivation in ND mice after 3 hours, whereas WD mice immune system was significantly upregulated. This suggests the need for early and more effective intervention in stroke patients with hypercholesterolemia, as even within therapeutic window, a similar overactivation pattern is expected.

It has been shown in other studies that neutrophils play a key role in hyperlipidemic mice three days after stroke, causing worse prognosis and more neuronal loss, which was attenuated after inhibition of neutrophil recruitment (Herz et al., 2015). Furthermore, it was recently found by our group that obese mice (with hyperlipidemia) had defects in brain vascularization, even without stroke induction, resulting in less vessel branch length and tortuosity (Spangenberg et al., 2023). Together, these data indicate the preconditioning effect of hyperlipidemia on brain vasculature, which is affected worse after stroke via neutrophils. As three hours is still within the therapeutic window, our current study proposes that patients with hyperlipidemia admitted at this time point may not benefit from classical stroke treatments as strongly as patients without hyperlipidemia, resulting in worse prognosis. Our study further underlines the importance of neutrophils in early response of immune system to stroke. Therefore, a better characterization of patient risk factors and comorbidities plays a crucial role in early stroke treatment from which patients could benefit more. Moreover, personalized medicine at admission should play a key role in the adjustment of acute stroke treatment including characterization of patient immune system and comorbidities. This characterization should be supported by a detailed understanding of stroke pathophysiology, which is beyond neuroprotection and re-canalization. Hence, further studies should also focus on the interaction of comorbidities, immune system and its early activation after stroke, which might cause infections and mortality.

The combination of the two subsets of the presented experiments propose a fundamental differential regulation of neutrophils after stroke in different pre-conditioned conditions, which might cause immunosuppression and mucosal barrier dysfunction. Hence, two

subsets of experiments might be combined in the future via investigating in detail the effect of neutrophils on gut immunity in mice with comorbidities. Furthermore, in the clinics, several parameters as comorbidities might be defined in different patient groups to measure IgA regulation after stroke. Future studies focusing on the role of neutrophils in IgA regulation process will be fundamental to understand whether certain immune cells, neutrophils, can cause cell death in different immune organs. Interventions aiming at these conditions might open new therapeutic possibilities to avoid infections in the clinics after stroke.

6. Summary

17 million people suffer from stroke every year. Among those, more than 50% of patients exhibit high cholesterol levels at admission, which makes hyperlipidemia one of the most common comorbidities. Furthermore, after stroke, about one third of patients show signs of infection. Yet, there is no targeted therapy for patients with hyperlipidemia, or no targeted therapy against infections and studies investigating these conditions are scarce. Hence, this study focuses on the most abundant mucosal antibody, Immunoglobulin A (IgA) and the effects of hyperlipidemia on immune system regulation after stroke.

In this study, it is shown that stroke reduces the numbers of B cells in Peyer's patches (PP), which might lead to the decreased levels of plasma IgA levels. This condition might make patients susceptible to infections, increasing morbidity and mortality. The negative correlation between neutrophil activation and plasma IgA levels can be a result of activated neutrophils, which causes PP B cell number and plasma IgA decrease, and it is crucial to understand the exact pathophysiological mechanisms and activation patterns of neutrophils. As most of the patients are introduced to stroke unit with comorbidities, the preclinical model of hyperlipidemia is utilized and these mice also show smaller numbers of B cells in PPs and reduced plasma IgA after stroke. These comorbidities might be related to worse outcome via induction of early neutrophil activation and PP B cell decrease. Neutrophils being early activators after stroke, our analysis and experimental paradigm show that the innate immune system is more activated, and more proinflammatory cytokines are released in Western Diet (WD) fed animals within the therapeutic window after stroke, causing significantly more damage in the brain. Preclinical studies focusing on early immune response in animals with comorbidities will be fundamental to find key therapeutic targets in stroke. As a result, targeting early innate immune response should be one of the keys aims in stroke treatment with more emphasis on patients with comorbidities. Mechanistic understanding for IgA regulation and the role of neutrophil extracellular traps (NETs) in this process might open a new path to develop new therapeutic targets.

Zusammenfassung

Jährlich leiden 17 Millionen Menschen an einem Schlaganfall, wobei mehr als 50% hohe Cholesterinspiegel aufweisen, was Hyperlipidämie zu einer der häufigsten Begleiterkrankungen macht. Etwa ein Drittel zeigt nach dem Schlaganfall Infektionszeichen. Trotzdem gibt es keine spezifische Therapie für Schlaganfallpatienten mit Hyperlipidämie oder gegen Infektionen und die Studien, die diese Zustände untersuchen, sind selten. Daher konzentriert sich diese Studie auf das am häufigsten vorkommende mukosale Antikörper, das Immunglobulin A (IgA), und die Auswirkungen von Hyperlipidämie auf die Immunsystemregulation nach einem Schlaganfall. In dieser Studie wird gezeigt, dass ein Schlaganfall die Anzahl der B-Zellen in Peyer'schen Plaques (PP) reduziert, was zu einem Rückgang der Plasmakonzentrationen von IgA führen könnte. Dieser Zustand könnte Patienten anfällig für Infektionen machen. Der Grund für die negative Korrelation zwischen Neutrophilenaktivierung und Plasma-IgA-Spiegeln kann auf aktivierte Neutrophile zurückzuführen sein, die zu einer PP-B-Zellzahl und einem Rückgang von Plasma-IgA führen. Es ist von entscheidender Bedeutung, die genauen pathophysiologischen Mechanismen und Aktivierungsmuster von Neutrophilen zu verstehen. Da die meisten Patienten auf der Schlaganfallstation erhöhte Cholesterinwerte zeigen, wird das präklinische Modell der Hyperlipidämie genutzt und auch diese Mäuse zeigen nach einem Schlaganfall kleinere Zahlen von B-Zellen in PPs und reduziertes Plasma-IgA. Frühzeitige Neutrophilenaktivierung könnte zu schlechteren Ergebnissen führen, da Neutrophile früh nach einem Schlaganfall aktiviert sind, zeigen unsere Analyse und unser experimentelles Paradigma, dass das angeborene Immunsystem stärker aktiviert ist und mehr proinflammatorische Zytokine in Tieren freigesetzt werden, die nach einem Schlaganfall eine westliche Diät (WD) erhalten, was zu signifikant mehr Schäden im Gehirn führt. Präklinische Studien, die sich auf die frühe Immunantwort bei Tieren mit Begleiterkrankungen konzentrieren, werden grundlegend sein, um Schlüsseltherapieziele bei Schlaganfällen zu finden. Daher sollte das Ziel der frühen angeborenen Immunantwort eines der Schlüsselziele in der Schlaganfallbehandlung sein, wobei mehr Wert auf Patienten mit Begleiterkrankungen gelegt wird. Ein mechanistisches Verständnis für die IgA-Regulation und die Rolle der Neutrophil Extracellular Traps (NETs) in diesem Prozess könnte einen neuen Weg eröffnen, um neue therapeutische Ziele zu entwickeln.

7. References

1. Alamowitch, S., Turc, G., Palaiodimou, L., Bivard, A., Cameron, A., De Marchis, G.M., Fromm, A., Korv, J., Roaldsen, M.B., Katsanos, A.H., and Tsivgoulis, G. (2023). European Stroke Organisation (ESO) expedited recommendation on tenecteplase for acute ischaemic stroke. Eur Stroke J 8, 8-54. 10.1177/23969873221150022.
2. Arnold, M., Liesirova, K., Broeg-Morvay, A., Meisterernst, J., Schlager, M., Mono, M.L., El-Koussy, M., Kagi, G., Jung, S., and Sarikaya, H. (2016). Dysphagia in Acute Stroke: Incidence, Burden and Impact on Clinical Outcome. PLoS One 11, e0148424. 10.1371/journal.pone.0148424.
3. Aubert, C.E., Kabeto, M., Kumar, N., and Wei, M.Y. (2022). Multimorbidity and long-term disability and physical functioning decline in middle-aged and older Americans: an observational study. BMC Geriatr 22, 910. 10.1186/s12877-022-03548-9.
4. Bathla, G., Ajmera, P., Mehta, P.M., Benson, J.C., Derdeyn, C.P., Lanzino, G., Agarwal, A., and Brinjikji, W. (2023). Advances in Acute Ischemic Stroke Treatment: Current Status and Future Directions. AJNR Am J Neuroradiol 44, 750-758. 10.3174/ajnr.A7872.
5. Benjamin, E.J., Muntner, P., Alonso, A., Bittencourt, M.S., Callaway, C.W., Carson, A.P., Chamberlain, A.M., Chang, A.R., Cheng, S., Das, S.R., Delling, F. N., Djousse, L., Elkind, M. S. V., Ferguson, J. F., Fornage, M., Jordan, L. C., Khan, S. S., Kissela, B. M., Knutson, K. L., Kwan, T. W., Lackland, D.T., Lewis, T.T., Lichtman, J.H., Longenecker, C.T., Loop, M.S., Lutsey, P.L., Martin, S.S., Matsushita, K., Moran, A.E., Mussolino, M.E., O'Flaherty, M., Pandey, A., Perak, A.M., Rosamond, W.D., Roth, G.A., Sampson, U.K.A., Satou, G.M., Schroeder, E.B., Shah, S.H., Spartano, N.L., Stokes, A., Tirschwell, D.L., Tsao, C.W., Turakhia, M.P., VanWagner, L.B., Wilkins, J.T., Wong, S.S., Virani, S.S.; American Heart Association Council on Epidemiology and Prevention Statistics Committee and Stroke Statistics Subcommittee (2019). Heart Disease and Stroke Statistics-2019 Update: A Report From the American Heart Association. Circulation 139, e56-e528. 10.1161/CIR.0000000000000659.

6. Berge, E., Whiteley, W., Audebert, H., De Marchis, G.M., Fonseca, A.C., Padiglioni, C., de la Ossa, N.P., Strbian, D., Tsivgoulis, G., and Turc, G. (2021). European Stroke Organisation (ESO) guidelines on intravenous thrombolysis for acute ischaemic stroke. Eur Stroke J 6, I-LXII. 10.1177/2396987321989865.
7. Blaszczak, A.M., Jalilvand, A., and Hsueh, W.A. (2021). Adipocytes, Innate Immunity and Obesity: A Mini-Review. Front Immunol 12, 650768. 10.3389/fimmu.2021.650768.
8. Bonkhoff, A.K., Hong, S., Bretzner, M., Schirmer, M.D., Regenhardt, R.W., Arsava, E.M., Donahue, K., Nardin, M., Dalca, A., Giese, A.K., Etherton M.R., Hancock B.L., Mocking S.J.T., McIntosh E., Attia J., Benavente O., Cole J.W., Donatti A., Griessenauer C., Heitsch L., Holmegaard L., Jood K., Jimenez-Conde J., Kittner S., Lemmens R., Levi C., McDonough C.W., Meschia J., Phuah C.L., Rolfs A., Ropele S., Rosand J., Roquer J., Rundek T., Sacco R.L., Schmidt R., Sharma P., Slowik A., Soederholm M., Sousa A., Stanne T.M., Strbian D., Tatlisumak T., Thijs V., Vagal A., Wasselius J., Woo D., Zand R., McArdle P., Worrall B.B., Jern C., Lindgren A.G., Maguire J., Golland P., Bzdok D., Wu O., Rost N.S. (2022). Association of Stroke Lesion Pattern and White Matter Hyperintensity Burden With Stroke Severity and Outcome. Neurology 99, e1364-e1379. 10.1212/WNL.0000000000200926.
9. Cai, W., Liu, S., Hu, M., Huang, F., Zhu, Q., Qiu, W., Hu, X., Colello, J., Zheng, S.G., and Lu, Z. (2020). Functional Dynamics of Neutrophils After Ischemic Stroke. Transl Stroke Res 11, 108-121. 10.1007/s12975-019-00694-y.
10. Chen, R., Kang, R., and Tang, D. (2022). The mechanism of HMGB1 secretion and release. Exp Mol Med 54, 91-102. 10.1038/s12276-022-00736-w.
11. Collaborators, G.B.D.S. (2021). Global, regional, and national burden of stroke and its risk factors, 1990-2019: a systematic analysis for the Global Burden of Disease Study 2019. Lancet Neurol 20, 795-820. 10.1016/S1474-4422(21)00252-0.
12. Dawson, J., Bejot, Y., Christensen, L.M., De Marchis, G.M., Dichgans, M., Hagberg, G., Heldner, M.R., Milionis, H., Li, L., Pezzella, F.R., Taylor Rowan, M., Tiu, C., and Webb, A. (2022). European Stroke Organisation (ESO) guideline on pharmacological interventions for long-term secondary prevention after ischaemic stroke or transient ischaemic attack. Eur Stroke J 7, I-II. 10.1177/23969873221100032.

13. Denorme, F., Portier, I., Rustad, J.L., Cody, M.J., de Araujo, C.V., Hoki, C., Alexander, M.D., Grandhi, R., Dyer, M.R., Neal, M.D., Majersik, J.J., Yost, C.C., and Campbell, R.A. (2022). Neutrophil extracellular traps regulate ischemic stroke brain injury. J Clin Invest 132. 10.1172/JCI154225.
14. Dirnagl, U., Iadecola, C., and Moskowitz, M.A. (1999). Pathobiology of ischaemic stroke: an integrated view. Trends Neurosci 22, 391-397. 10.1016/s0166-2236(99)01401-0.
15. Drechsler, M., Megens, R.T., van Zandvoort, M., Weber, C., and Soehnlein, O. (2010). Hyperlipidemia-triggered neutrophilia promotes early atherosclerosis. Circulation 122, 1837-1845. 10.1161/CIRCULATIONAHA.110.961714.
16. Du, W., Zhao, X., Wang, Y., Pan, Y., Liu, G., Wang, A., Ji, R., Liu, L., Gu, H., Dong, K., Wang, P., Wang, Y., and China National Stroke Registry (CNSR) investigators (2020). Gastrointestinal bleeding during acute ischaemic stroke hospitalisation increases the risk of stroke recurrence. Stroke Vasc Neurol 5, 116-120. 10.1136/svn-2019-000314.
17. ElAli, A., Doeppner, T.R., Zechariah, A., and Hermann, D.M. (2011). Increased blood-brain barrier permeability and brain edema after focal cerebral ischemia induced by hyperlipidemia: role of lipid peroxidation and calpain-1/2, matrix metalloproteinase-2/9, and RhoA overactivation. Stroke 42, 3238-3244. 10.1161/STROKEAHA.111.615559.
18. Feigin, V.L., Roth, G.A., Naghavi, M., Parmar, P., Krishnamurthi, R., Chugh, S., Mensah, G.A., Norrving, B., Shiue, I., Ng, M., Estep, K., Cercy, K., Murray, C.J.L., Forouzanfar, M.H., and Global Burden of Diseases, Injuries and Risk Factors Study 2013 and Stroke Experts Writing Group (2016). Global burden of stroke and risk factors in 188 countries, during 1990-2013: a systematic analysis for the Global Burden of Disease Study 2013. Lancet Neurol 15, 913-924. 10.1016/S1474-4422(16)30073-4.
19. Fu, J. (2019). Factors affecting the occurrence of gastrointestinal bleeding in acute ischemic stroke patients. Medicine (Baltimore) 98, e16312. 10.1097/MD.0000000000016312.

20. Gaffen, S.L., Jain, R., Garg, A.V., and Cua, D.J. (2014). The IL-23-IL-17 immune axis: from mechanisms to therapeutic testing. Nat Rev Immunol 14, 585-600. 10.1038/nri3707.
21. Gaynor, E., Rohde, D., Large, M., Mellon, L., Hall, P., Brewer, L., Conway, O., Hickey, A., Bennett, K., Dolan, E., Callaly, E., and Williams, D. (2018). Cognitive Impairment, Vulnerability, and Mortality Post Ischemic Stroke: A Five-Year Follow-Up of the Action on Secondary Prevention Interventions and Rehabilitation in Stroke (ASPIRE-S) Cohort. J Stroke Cerebrovasc Dis 27, 2466-2473. 10.1016/j.jstrokecerebrovasdis.2018.05.002.
22. Gelderblom, M., Leypoldt, F., Steinbach, K., Behrens, D., Choe, C.U., Siler, D.A., Arumugam, T.V., Orthey, E., Gerloff, C., Tolosa, E., and Magnus, T. (2009). Temporal and spatial dynamics of cerebral immune cell accumulation in stroke. Stroke 40, 1849-1857. 10.1161/STROKEAHA.108.534503.
23. Grossmann, I., Rodriguez, K., Soni, M., Joshi, P.K., Patel, S.C., Shreya, D., Zamora, D.I., Patel, G.S., and Sange, I. (2021). Stroke and Pneumonia: Mechanisms, Risk Factors, Management, and Prevention. Cureus 13, e19912. 10.7759/cureus.19912.
24. Haak, B.W., Westendorp, W.F., van Engelen, T.S.R., Brands, X., Brouwer, M.C., Vermeij, J.D., Hugenholtz, F., Verhoeven, A., Derks, R.J., Giera, M., Nederkoorn, P.J., de Vos, W.M., van de Beek, D., and Wiersinga, W. J. (2021). Disruptions of Anaerobic Gut Bacteria Are Associated with Stroke and Post-stroke Infection: a Prospective Case-Control Study. Transl Stroke Res 12, 581-592. 10.1007/s12975-020-00863-4.
25. Hand, T.W., and Reboldi, A. (2021). Production and Function of Immunoglobulin A. Annu Rev Immunol 39, 695-718. 10.1146/annurev-immunol-102119-074236.
26. Hara, S., Sasaki, T., Satoh-Takayama, N., Kanaya, T., Kato, T., Takikawa, Y., Takahashi, M., Tachibana, N., Kim, K.S., Surh, C.D., and Ohno, H. (2019). Dietary Antigens Induce Germinal Center Responses in Peyer's Patches and Antigen-Specific IgA Production. Front Immunol 10, 2432. 10.3389/fimmu.2019.02432.
27. Herz, J., Hagen, S.I., Bergmuller, E., Sabellek, P., Gothert, J.R., Buer, J., Hansen, W., Hermann, D.M., and Doeppner, T.R. (2014). Exacerbation of ischemic brain injury in hypercholesterolemic mice is associated with pronounced changes in peripheral and cerebral immune responses. Neurobiol Dis 62, 456-468. 10.1016/j.nbd.2013.10.022.

28. Herz, J., Sabellek, P., Lane, T.E., Gunzer, M., Hermann, D.M., and Doeppner, T.R. (2015). Role of Neutrophils in Exacerbation of Brain Injury After Focal Cerebral Ischemia in Hyperlipidemic Mice. Stroke 46, 2916-2925. 10.1161/STROKEAHA.115.010620.
29. Hintze, K.J., Benninghoff, A.D., Cho, C.E., and Ward, R.E. (2018). Modeling the Western Diet for Preclinical Investigations. Adv Nutr 9, 263-271. 10.1093/advances/nmy002.
30. Hu, W., Kong, X., Wang, H., Li, Y., and Luo, Y. (2022). Ischemic stroke and intestinal flora: an insight into brain-gut axis. Eur J Med Res 27, 73. 10.1186/s40001-022-00691-2.
31. Huang, Y., Chen, S., Luo, Y., and Han, Z. (2020). Crosstalk between Inflammation and the BBB in Stroke. Curr Neuropharmacol 18, 1227-1236. 10.2174/1570159X18666200620230321.
32. Huus, K.E., Petersen, C., and Finlay, B.B. (2021). Diversity and dynamism of IgA-microbiota interactions. Nat Rev Immunol 21, 514-525. 10.1038/s41577-021-00506-1.
33. Jang, D.I., Lee, A.H., Shin, H.Y., Song, H.R., Park, J.H., Kang, T.B., Lee, S.R., and Yang, S.H. (2021). The Role of Tumor Necrosis Factor Alpha (TNF-alpha) in Autoimmune Disease and Current TNF-alpha Inhibitors in Therapeutics. Int J Mol Sci 22. 10.3390/ijms22052719.
34. Jickling, G.C., Liu, D., Ander, B.P., Stamova, B., Zhan, X., and Sharp, F.R. (2015). Targeting neutrophils in ischemic stroke: translational insights from experimental studies. J Cereb Blood Flow Metab 35, 888-901. 10.1038/jcbfm.2015.45.
35. Jin, F., Hagemann, N., Sun, L., Wu, J., Doeppner, T.R., Dai, Y., and Hermann, D.M. (2018). High-density lipoprotein (HDL) promotes angiogenesis via S1P3-dependent VEGFR2 activation. Angiogenesis 21, 381-394. 10.1007/s10456-018-9603-z.
36. Kane, E., and Ward, N.S. (2021). Neurobiology of Stroke Recovery. In Clinical Pathways in Stroke Rehabilitation: Evidence-based Clinical Practice Recommendations, T. Platz, ed. pp. 1-13. 10.1007/978-3-030-58505-1_1.
37. Kang, L., Yu, H., Yang, X., Zhu, Y., Bai, X., Wang, R., Cao, Y., Xu, H., Luo, H., Lu, L., Shi, M.J., Tian, Y., Fan, W., and Zhao, B.Q. (2020). Neutrophil extracellular traps

released by neutrophils impair revascularization and vascular remodeling after stroke. Nat Commun 11, 2488. 10.1038/s41467-020-16191-y.

38. Kilkenny, C., Browne, W.J., Cuthi, I., Emerson, M., and Altman, D.G. (2012). Improving bioscience research reporting: the ARRIVE guidelines for reporting animal research. Vet Clin Pathol 41, 27-31. 10.1111/j.1939-165X.2012.00418.x.
39. Komban, R.J., Stromberg, A., Biram, A., Cervin, J., Lebrero-Fernandez, C., Mabbott, N., Yrlid, U., Shulman, Z., Bemark, M., and Lycke, N. (2019). Activated Peyer's patch B cells sample antigen directly from M cells in the subepithelial dome. Nat Commun 10, 2423. 10.1038/s41467-019-10144-w.
40. Kumar, S., Selim, M.H., and Caplan, L.R. (2010). Medical complications after stroke. Lancet Neurol 9, 105-118. 10.1016/S1474-4422(09)70266-2.
41. Lakhan, S.E., Kirchgessner, A., and Hofer, M. (2009). Inflammatory mechanisms in ischemic stroke: therapeutic approaches. J Transl Med 7, 97. 10.1186/1479-5876-7-97.
42. Laridan, E., Denorme, F., Desender, L., Francois, O., Andersson, T., Deckmyn, H., Vanhoorelbeke, K., and De Meyer, S.F. (2017). Neutrophil extracellular traps in ischemic stroke thrombi. Ann Neurol 82, 223-232. 10.1002/ana.24993.
43. Lee, K.M.C., Achuthan, A.A., and Hamilton, J.A. (2020). GM-CSF: A Promising Target in Inflammation and Autoimmunity. Immunotargets Ther 9, 225-240. 10.2147/ITT.S262566.
44. Li, J., Yuan, M., Liu, Y., Zhao, Y., Wang, J., and Guo, W. (2017). Incidence of constipation in stroke patients: A systematic review and meta-analysis. Medicine (Baltimore) 96, e7225. 10.1097/MD.0000000000007225.
45. Li, Y., and Zhang, J. (2021). Animal models of stroke. Animal Model Exp Med 4, 204-219. 10.1002/ame2.12179.
46. Li, Y., Jin, L., and Chen, T. (2020). The Effects of Secretory IgA in the Mucosal Immune System. Biomed Res Int 2020, 2032057. 10.1155/2020/2032057.
47. Lin, Y.T., Chen, H.D., Ai, Q.D., Yang, Y.T., Zhang, Z., Chu, S.F., and Chen, N.H. (2023). Characteristics and pathogenesis of chemokines in the post-stroke stage. Int Immunopharmacol 116, 109781. 10.1016/j.intimp.2023.109781.

48. Liu, C.C., Liu, C.C., Kanekiyo, T., Xu, H., and Bu, G. (2013). Apolipoprotein E and Alzheimer disease: risk, mechanisms and therapy. Nat Rev Neurol 9, 106-118. 10.1038/nrneurol.2012.263.
49. Liu, F., and McCullough, L.D. (2014). The middle cerebral artery occlusion model of transient focal cerebral ischemia. Methods Mol Biol 1135, 81-93. 10.1007/978-1-4939-0320-7_7.
50. Lycke, N.Y., and Bemark, M. (2012). The role of Peyer's patches in synchronizing gut IgA responses. Front Immunol 3, 329. 10.3389/fimmu.2012.00329.
51. Marshall, I.J., Wang, Y., Crichton, S., McKevitt, C., Rudd, A.G., and Wolfe, C.D. (2015). The effects of socioeconomic status on stroke risk and outcomes. Lancet Neurol 14, 1206-1218. 10.1016/S1474-4422(15)00200-8.
52. Matur, A.V., Candelario-Jalil, E., Paul, S., Karamyan, V.T., Lee, J.D., Pennypacker, K., and Fraser, J.F. (2022). Translating Animal Models of Ischemic Stroke to the Human Condition. Transl Stroke Res. 10.1007/s12975-022-01082-9.
53. Mayer, E.A. (2000). The neurobiology of stress and gastrointestinal disease. Gut 47, 861-869. 10.1136/gut.47.6.861.
54. Merriman, N.A., Sexton, E., Donnelly, N.A., McCabe, G., Walsh, M.E., Rohde, D., Gorman, A., Jeffares, I., Pender, N., Williams, D., Horgan, F., Doyle, F., Wren, M.A., Bennett, K.E., and Hickey, A. (2018). Managing cognitive impairment following stroke: protocol for a systematic review of non-randomised controlled studies of psychological interventions. BMJ Open 8, e019001. 10.1136/bmjopen-2017-019001.
55. Nelson, M.L.A., McKellar, K.A., Yi, J., Kelloway, L., Munce, S., Cott, C., Hall, R., Fortin, M., Teasell, R., and Lyons, R. (2017). Stroke rehabilitation evidence and comorbidity: a systematic scoping review of randomized controlled trials. Top Stroke Rehabil 24, 374-380. 10.1080/10749357.2017.1282412.
56. Nelson, R.H. (2013). Hyperlipidemia as a risk factor for cardiovascular disease. Prim Care 40, 195-211. 10.1016/j.pop.2012.11.003.
57. Neumann, J., Riek-Burchardt, M., Herz, J., Doeppner, T.R., Konig, R., Hutten, H., Etemire, E., Mann, L., Klingberg, A., Fischer, T., Görtler, M.W., Heinze, H.J., Reichardt, P., Schraven, B., Hermann, D.M., Reymann, K.G., and Gunzer, M. (2015). Very-late-antigen-4 (VLA-4)-mediated brain invasion by neutrophils leads to

interactions with microglia, increased ischemic injury and impaired behavior in experimental stroke. Acta Neuropathol 129, 259-277. 10.1007/s00401-014-1355-2.

58. O'Donnell, M.J., Chin, S.L., Rangarajan, S., Xavier, D., Liu, L., Zhang, H., Rao-Melacini, P., Zhang, X., Pais, P., Agapay, S., Lopez-Jaramillo, P., Damasceno, A., Langhorne, P., McQueen, M.J., Rosengren, A., Dehghan, M., Hankey, G.J., Dans, A.L., Elsayed, A., Avezum, A., Mondo, C., Diener, H.C., Ryglewicz, D., Czlonkowska, A., Pogosova, N., Weimar, C., Iqbal, R., Diaz, R., Yusoff, K., Yusufali, A., Oguz, A., Wang, X., Penaherrera, E., Lanas, F., Ogah, O.S., Ogunniyi, A., Iversen, H.K., Malaga, G., Rumboldt, Z., Oveisgharan, S., Al Hussain, F., Magazi, D., Nilanont, Y., Ferguson, J., Pare, G., Yusuf, S.; INTERSTROKE investigators. (2016). Global and regional effects of potentially modifiable risk factors associated with acute stroke in 32 countries (INTERSTROKE): a case-control study. Lancet 388, 761-775. 10.1016/S0140-6736(16)30506-2.
59. Papayannopoulos, V. (2018). Neutrophil extracellular traps in immunity and disease. Nat Rev Immunol 18, 134-147. 10.1038/nri.2017.105.
60. Pati, S., Swain, S., Knottnerus, J.A., Metsemakers, J.F.M., and van den Akker, M. (2019). Health related quality of life in multimorbidity: a primary-care based study from Odisha, India. Health Qual Life Outcomes 17, 116. 10.1186/s12955-019-1180-3.
61. Pawlinski, R. (2016). Platelet HMGB1: the venous clot coordinator. Blood 128, 2376-2378. 10.1182/blood-2016-09-738740.
62. Pittman, K., and Kubes, P. (2013). Damage-associated molecular patterns control neutrophil recruitment. J Innate Immun 5, 315-323. 10.1159/000347132.
63. Poisson, S.N., Johnston, S.C., and Josephson, S.A. (2010). Urinary tract infections complicating stroke: mechanisms, consequences, and possible solutions. Stroke 41, e180-184. 10.1161/STROKEAHA.109.576413.
64. Prados-Torres, A., Calderon-Larranaga, A., Hancco-Saavedra, J., Poblador-Plou, B., and van den Akker, M. (2014). Multimorbidity patterns: a systematic review. J Clin Epidemiol 67, 254-266. 10.1016/j.jclinepi.2013.09.021.
65. Quinn, T.J., Richard, E., Teuschl, Y., Gattringer, T., Hafdi, M., O'Brien, J.T., Merriman, N., Gillebert, C., Huyglier, H., Verdelho, A., Schmidt, R., Ghaziani, E., Forchammer, H., Pendlebury, S.T., Bruffaerts, R., Mijajlovic, M., Drozdowska, B.A.,

Ball, E., & Markus, H.S. (2021). European Stroke Organisation and European Academy of Neurology joint guidelines on post-stroke cognitive impairment. Eur Stroke J 6, I-XXXVIII. 10.1177/23969873211042192.

66. Reboldi, A., and Cyster, J.G. (2016). Peyer's patches: organizing B-cell responses at the intestinal frontier. Immunol Rev 271, 230-245. 10.1111/imr.12400.
67. Renier, N., Wu, Z., Simon, D.J., Yang, J., Ariel, P., and Tessier-Lavigne, M. (2014). iDISCO: a simple, rapid method to immunolabel large tissue samples for volume imaging. Cell 159, 896-910. 10.1016/j.cell.2014.10.010.
68. Restrepo, L., Bang, O.Y., Ovbiagele, B., Ali, L., Kim, D., Liebeskind, D.S., Starkman, S., Vinuela, F., Duckwiler, G.R., Jahan, R., and Saver, J.L. (2009). Impact of hyperlipidemia and statins on ischemic stroke outcomes after intra-arterial fibrinolysis and percutaneous mechanical embolectomy. Cerebrovasc Dis 28, 384-390. 10.1159/000235625.
69. Rofes, L., Muriana, D., Palomeras, E., Vilardell, N., Palomera, E., Alvarez-Berdugo, D., Casado, V., and Clave, P. (2018). Prevalence, risk factors and complications of oropharyngeal dysphagia in stroke patients: A cohort study. Neurogastroenterol Motil, e13338. 10.1111/nmo.13338.
70. Rolfes, L., Riek-Burchardt, M., Pawlitzki, M., Minnerup, J., Bock, S., Schmidt, M., Meuth, S.G., Gunzer, M., and Neumann, J. (2021). Neutrophil granulocytes promote flow stagnation due to dynamic capillary stalls following experimental stroke. Brain Behav Immun 93, 322-330. 10.1016/j.bbi.2021.01.011.
71. Roth, S., Cao, J., Singh, V., Tiedt, S., Hundeshagen, G., Li, T., Boehme, J.D., Chauhan, D., Zhu, J., Ricci, A., Gorka, O., Asare, Y., Yang, J., Lopez, M.S., Rehberg, M., Bruder, D., Zhang, S., Groß, O., Dichgans, M., Hornung, V., Liesz, A. (2021). Post-injury immunosuppression and secondary infections are caused by an AIM2 inflammasome-driven signaling cascade. Immunity 54, 648-659 e648. 10.1016/j.immuni.2021.02.004.
72. Roth, W.H., Cai, A., Zhang, C., Chen, M.L., Merkler, A.E., and Kamel, H. (2020). Gastrointestinal Disorders and Risk of First-Ever Ischemic Stroke. Stroke 51, 3577-3583. 10.1161/STROKEAHA.120.030643.
73. Sacco, R.L., Diener, H.C., Yusuf, S., Cotton, D., Ounpuu, S., Lawton, W.A., Palesch, Y., Martin, R.H., Albers, G.W., Bath, P., Bornstein, N., Chan, B.P., Chen, S.T.,

Cunha, L., Dahlöf, B., De Keyser, J., Donnan, G.A., Estol, C., Gorelick, P., Gu, V., Hermansson, K., Hilbrich, L., Kaste, M., Lu, C., Machnig, T., Pais, P., Roberts, R., Skvortsova, V., Teal, P., Toni, D., Vandermaelen, C., Voigt, T., Weber, M., Yoon, B.W.; PRoFESS Study Group. (2008). Aspirin and extended-release dipyridamole versus clopidogrel for recurrent stroke. N Engl J Med 359, 1238-1251. 10.1056/NEJMoa0805002.

74. Sharifi-Rad, M., Anil Kumar, N.V., Zucca, P., Varoni, E.M., Dini, L., Panzarini, E., Rajkovic, J., Tsouh Fokou, P.V., Azzini, E., Peluso, I., Prakash Mishra, A., Nigam, M., El Rayess, Y., Beyrouthy, M. E., Polito, L., Iriti, M., Martins, N., Martorell, M., Docea, A. O., Setzer, W. N., Calina, D., Cho, W.C., Sharifi-Rad, J. (2020). Lifestyle, Oxidative Stress, and Antioxidants: Back and Forth in the Pathophysiology of Chronic Diseases. Front Physiol 11, 694. 10.3389/fphys.2020.00694.
75. She, R., Yan, Z., Hao, Y., Zhang, Z., Du, Y., Liang, Y., Vetrano, D.L., Dekker, J., Bai, B., Lau, J.T.F., and Qiu, C. (2022). Comorbidity in patients with first-ever ischemic stroke: Disease patterns and their associations with cognitive and physical function. Front Aging Neurosci 14, 887032. 10.3389/fnagi.2022.887032.
76. Silk, E., Zhao, H., Weng, H., and Ma, D. (2017). The role of extracellular histone in organ injury. Cell Death Dis 8, e2812. 10.1038/cddis.2017.52.
77. Silvestre-Roig, C., Braster, Q., Wichapong, K., Lee, E.Y., Teulon, J.M., Berrebeh, N., Winter, J., Adrover, J.M., Santos, G.S., Froese, A., Lemnitzer, P., Ortega-Gómez, A., Chevre, R., Marschner, J., Schumski, A., Winter, C., Perez-Olivares, L., Pan, C., Paulin, N., Schoufour, T., Hartwig, H., González-Ramos, S., Kamp, F., Megens, R.T.A., Mowen, K.A., Gunzer, M., Maegdefessel, L., Hackeng, T., Lutgens, E., Daemen, M., von Blume, J., Anders, H.J., Nikolaev, V.O., Pellequer, J.L., Weber, C., Hidalgo, A., Nicolaes, G.A.F., Wong, G.C.L., Soehnlein, O. (2019). Externalized histone H4 orchestrates chronic inflammation by inducing lytic cell death. Nature 569, 236-240. 10.1038/s41586-019-1167-6.
78. Singh, V., Roth, S., Llovera, G., Sadler, R., Garzetti, D., Stecher, B., Dichgans, M., and Liesz, A. (2016). Microbiota Dysbiosis Controls the Neuroinflammatory Response after Stroke. J Neurosci 36, 7428-7440. 10.1523/JNEUROSCI.1114-16.2016.

79. Spangenberg, P., Hagemann, N., Squire, A., Forster, N., Krauss, S.D., Qi, Y., Mohamud Yusuf, A., Wang, J., Gruneboom, A., Kowitz, L., Korste, S., Totzeck, M., Cibir, Z., Tuz, A. A., Singh, V., Siemes, D., Struensee, L., Engel, D. R., Ludewig, P., Martins Nascentes Melo, L., Helfrich, I., Chen, J., Gunzer, M., Hermann, D.M., Mosig, A. (2023). Rapid and fully automated blood vasculature analysis in 3D light-sheet image volumes of different organs. Cell Rep Methods 3, 100436. 10.1016/j.crmeth.2023.100436.
80. Sposito, B., Broggi, A., Pandolfi, L., Crotta, S., Clementi, N., Ferrarese, R., Sisti, S., Criscuolo, E., Spreafico, R., Long, J.M., Ambrosi, A., Liu, E., Frangipane, V., Saracino, L., Bozzini, S., Marongiu, L., Facchini, F. A., Bottazzi, A., Fossali, T., Colombo, R., Clementi, M., Tagliabue, E., Chou, J., Pontiroli, A.E., Meloni, F., Wack, A., Mancini, N., Zanoni, I. (2021). The interferon landscape along the respiratory tract impacts the severity of COVID-19. Cell 184, 4953-4968 e4916. 10.1016/j.cell.2021.08.016.
81. Stroke Prevetion by Aggressive Reduction in Cholestrol Levels, I., Karam, J.G., Loney-Hutchinson, L., and McFarlane, S.I. (2008). High-dose atorvastatin after stroke or transient ischemic attack: The Stroke Prevention by Aggressive Reduction in Cholesterol Levels (SPARCL) Investigators. J Cardiometab Syndr 3, 68-69. 10.1111/j.1559-4572.2008.07967.x.
82. Sugiyama, S., Sasaki, T., Tanaka, H., Yan, H., Ikegami, T., Kanki, H., Nishiyama, K., Beck, G., Gon, Y., Okazaki, S., Todo, K., Tamura, A., Tsukita, S., Mochizuki, H. (2023). The tight junction protein occludin modulates blood-brain barrier integrity and neurological function after ischemic stroke in mice. Sci Rep 13, 2892. 10.1038/s41598-023-29894-1.
83. Sun, S., Duan, Z., Wang, X., Chu, C., Yang, C., Chen, F., Wang, D., Wang, C., Li, Q., and Ding, W. (2021). Neutrophil extracellular traps impair intestinal barrier functions in sepsis by regulating TLR9-mediated endoplasmic reticulum stress pathway. Cell Death Dis 12, 606. 10.1038/s41419-021-03896-1.
84. Tan, C., Wu, Q., Wang, H., Gao, X., Xu, R., Cui, Z., Zhu, J., Zeng, X., Zhou, H., He, Y., and Yin, J. (2021). Dysbiosis of Gut Microbiota and Short-Chain Fatty Acids in Acute Ischemic Stroke and the Subsequent Risk for Poor Functional Outcomes. JPEN J Parenter Enteral Nutr 45, 518-529. 10.1002/jpen.1861.

85. Towfighi, A., Ovbiagele, B., El Husseini, N., Hackett, M.L., Jorge, R.E., Kissela, B.M., Mitchell, P.H., Skolarus, L.E., Whooley, M.A., Williams, L.S., American Heart Association Stroke Council (2017). Poststroke Depression: A Scientific Statement for Healthcare Professionals From the American Heart Association/American Stroke Association. Stroke 48, e30-e43. 10.1161/STR.0000000000000113.
86. Tsourouktsoglou, T.D., Warnatsch, A., Ioannou, M., Hoving, D., Wang, Q., and Papayannopoulos, V. (2020). Histones, DNA, and Citrullination Promote Neutrophil Extracellular Trap Inflammation by Regulating the Localization and Activation of TLR4. Cell Rep 31, 107602. 10.1016/j.celrep.2020.107602.
87. Turc, G., Bhogal, P., Fischer, U., Khatri, P., Lobotesis, K., Mazighi, M., Schellinger, P.D., Toni, D., de Vries, J., White, P., and Fiehler, J. (2023). European Stroke Organisation (ESO) - European Society for Minimally Invasive Neurological Therapy (ESMINT) Guidelines on Mechanical Thrombectomy in Acute Ischemic Stroke. J Neurointerv Surg 15, e8. 10.1136/neurintsurg-2018-014569.
88. Urban, C.F., Ermert, D., Schmid, M., Abu-Abed, U., Goosmann, C., Nacken, W., Brinkmann, V., Jungblut, P.R., and Zychlinsky, A. (2009). Neutrophil extracellular traps contain calprotectin, a cytosolic protein complex involved in host defense against Candida albicans. PLoS Pathog 5, e1000639. 10.1371/journal.ppat.1000639.
89. Victora, G.D., and Nussenzweig, M.C. (2022). Germinal Centers. Annu Rev Immunol 40, 413-442. 10.1146/annurev-immunol-120419-022408.
90. Wang, Y.R., Cui, W.Q., Wu, H.Y., Xu, X.D., and Xu, X.Q. (2023). The role of T cells in acute ischemic stroke. Brain Res Bull 196, 20-33. 10.1016/j.brainresbull.2023.03.005.
91. Watanabe, Y., Nagai, Y., Honda, H., Okamoto, N., Yanagibashi, T., Ogasawara, M., Yamamoto, S., Imamura, R., Takasaki, I., Hara, H., Sasahara, M., Arita, M., Hida, S., Taniguchi, S., Suda, T., Takatsu, K. (2019). Bidirectional crosstalk between neutrophils and adipocytes promotes adipose tissue inflammation. FASEB J 33, 11821-11835. 10.1096/fj.201900477RR.
92. Xia, G.H., You, C., Gao, X.X., Zeng, X.L., Zhu, J.J., Xu, K.Y., Tan, C.H., Xu, R.T., Wu, Q.H., Zhou, H.W., He, Y., and Yin, J. (2019). Stroke Dysbiosis Index (SDI) in Gut Microbiome Are Associated With Brain Injury and Prognosis of Stroke. Front Neurol 10, 397. 10.3389/fneur.2019.00397.

93. Yaghi, S., and Elkind, M.S. (2015). Lipids and Cerebrovascular Disease: Research and Practice. Stroke 46, 3322-3328. 10.1161/STROKEAHA.115.011164.
94. Yin, D., Wang, C., Qi, Y., Wang, Y.C., Hagemann, N., Mohamud Yusuf, A., Dzyubenko, E., Kaltwasser, B., Tertel, T., Giebel, B., Gunzer, M., Popa-Wagner, A., Doeppner, T. R., Hermann, D.M. (2023). Neural precursor cell delivery induces acute post-ischemic cerebroprotection, but fails to promote long-term stroke recovery in hyperlipidemic mice due to mechanisms that include pro-inflammatory responses associated with brain hemorrhages. J Neuroinflammation 20, 210. 10.1186/s12974-023-02894-8.
95. Yun, S.H., Sim, E.H., Goh, R.Y., Park, J.I., and Han, J.Y. (2016). Platelet Activation: The Mechanisms and Potential Biomarkers. Biomed Res Int 2016, 9060143. 10.1155/2016/9060143.
96. Zechariah, A., ElAli, A., Hagemann, N., Jin, F., Doeppner, T.R., Helfrich, I., Mies, G., and Hermann, D.M. (2013). Hyperlipidemia attenuates vascular endothelial growth factor-induced angiogenesis, impairs cerebral blood flow, and disturbs stroke recovery via decreased pericyte coverage of brain endothelial cells. Arterioscler Thromb Vasc Biol 33, 1561-1567. 10.1161/ATVBAHA.112.300749.
97. Zhang, D., Ren, J., Luo, Y., He, Q., Zhao, R., Chang, J., Yang, Y., and Guo, Z.N. (2021). T Cell Response in Ischemic Stroke: From Mechanisms to Translational Insights. Front Immunol 12, 707972. 10.3389/fimmu.2021.707972.
98. Zhu, H., Hu, S., Li, Y., Sun, Y., Xiong, X., Hu, X., Chen, J., and Qiu, S. (2022). Interleukins and Ischemic Stroke. Front Immunol 13, 828447. 10.3389/fimmu.2022.828447.

8. Attachment

8.1. List of abbreviations

°C	degree Celcius
µm	micrometer
3D	three dimensional
AdipoR1	adiponectin receptor 1
AdipoR2	adiponectin receptor 2
AF	autoflorescence
ANOVA	analysis of variance
APC	antigen presenting cell
ApoE	Apolipoprotein E
APRIL	A proliferation inducing ligand
ATP	adenosine triphosphate
BAFF	B cell activating factor
BAL	bronchoalveolar lavage
BBB	blood-brain barrier
BM	bone marroy
BSA	bovine serum albumin
CBF	cerebral blood flow
CCA	common carotid artery
CCL	chemokine C-C motif
CD	cluster of differentiation
cfDNA	cell free DNA
citH3	citrullinated Histone-3
CT	computerized tomography
CXCL1	chemokine C-X-C motif ligand 1
CXCL10	chemokine C-X-C motif ligand 10
CXCL2	chemokine C-X-C motif ligand 2
CXCR2	CXC motif receptor 2
DAMP	damage associated molecular pattern

DNA	deoxyribonucleic acid
ECA	external carotid artery
ECI	ethyl cinnamate
ECM	extracellular matrix
EDTA	ethylenediaminetetraacetic acid
ELISA	enzyme-linked immunosorbent assay
ESO	European Stroke Organisation
EtOH	ethanol
FACS	fluorescence activated cell sorting
FFA	free fatty acid
GALT	gut associated lymphoid tissue
GC	germinal center
G-CSF	granulocyte colony stimulating factor
GIT	gastrointestinal tract
GM-CSF	granulocyte-macrophage colony-stimulating factor
GPR	G protein coupled receptor
HDL	high density lipoprotein
HMGB1	high mobility group box 1
HRP	horse radish peroxidase
ICA	internal carotid artery
ICAM-1	intercellular adhesion molecule-1
IFN-γ	interferon-γ
IgA	Immunoglobulin A
IL-17	interleukin 17
IL-1β	interleukin-1β
ILF	isolated lymphoid follicle
LDF	laser doppler flow
LDL	low density lipoprotein
LP	lamina propria
LSFM	light-sheet fluorescence microscopy
Ly6	lymphocyte antigen 6 family
MACS	magnetic activated cell sorting

MCA	middle cerebral artery
MCP-1	monocyte chemoattractant protein
MHC	major histocompatibility complex
min	minutes
mLN	mesenteric lymph node
mm	millimeter
MMP	matrix metalloproteinase
MPO	myeloperoxidase
MPS	mononuclear phagocyte system
NADPH	nicotinamide adenine dinucleotide phosphate
NE	neutrophil elastase
NET	neutrophil extracellular trap
NIHSS	National Institutes of Health Stroke Scale
NLR	NOD-like receptor
nm	nanometer
NMDA	N-methyl-D-aspartate
NO	nitric oxide
PBS	phosphate-buffered saline
PC	plasma cell
PFA	paraformaldehyde
PKC	protein kinase C
PLA2	phospholipase A2
PMN	polymorphonuclear neutrophil
PP	Peyer's patch
PRR	pattern recognition receptor
RAGE	receptor for advanced glycation end products
RBC	red blood cell
ROS	reactive oxygen species
rpm	revolutions pre minute
s.c.	subcutaneous
SED	subepithelial dome
SIgA	secretory IgA

Th	helper T cell
TLR	Toll-like receptor
tMCAO	transient middle cerebral artery occlusion
TNF-α	tumor necrosis factor-α
tPA	tissue plasminogen activator
Treg	regulatory T cell
VCAM	vascular adhesion molecule-1
vWF	von Willebrand factor
WD	Western Diet
WT	wild type

8.2. List of tables

8.3. List of figures

9. Acknowledgements

I would like to express my sincere gratitude to Prof. Dr. Matthias Gunzer and Prof. Dr. Dirk Hermann for giving me the opportunity to switch from clinical daily routine to a completely different field of research. Their support for each of my ideas has been a great motivation to continue in times of frustration and tiredness. A special thanks to Matthias, for both teaching me how to ask the right questions in experimental design and making every technique available to use and learn.

I want to give my deepest appreciation to Dr. Vikramjeet Singh, who patiently showed me every technique and experimental paradigm, never getting tired of my questions. Without Vikram's patience and support, this thesis and degree would not have been possible.

I am grateful to all the students that I supervised, who helped me during experiments and also asked me all the questions that enhanced our collective learning. A thesis without the joy of teaching would not be complete.

I appreciate the support of all the members of AG Gunzer and AG Hermann, who were always there to help, discuss and share a coffee.

For all the discussions, brainstorming sessions, experiment designs, presentation practices at all possible times, not giving up on my never-ending experiment days, not letting me run away from research and most importantly, for being best partner in wine and life, thank you, Buse.

Last but not least, from my first step as a child to going abroad to follow my dreams, thank you mom for teaching me to be my best, and answering all the "why" questions I ask. Thank you, dad, for giving me confusing answers when I was a kid, fostering the joy of confusion and the will to learn. And Egemen, thank you for helping me understand that it is impossible to know all the answers, and for teaching me the value of saying "I don't know" to have to joy of learning together alongside you.

10. Curriculum Vitae

“The curriculum vitae is not included in the online version for data protection reasons.”